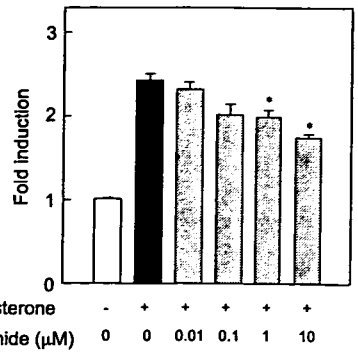

Fig. 5. The effect of nilutamide on *trans*-activation of the rOCT2 promoter (−3036/+242) by rAR in the presence of testosterone. Constructs were transiently transfected into LLC-PK_1 cells with rAR and pRL-TK. The cells were cultured for 43 h with vehicle and 10 nM testosterone in the absence or presence of various concentrations of nilutamide, and luciferase activity was measured. Firefly luciferase activity was normalized to *Renilla* luciferase activity. Each column represents the mean ± SE of three independent experiments. $*p < 0.05$, significantly different from testosterone (+) in the absence of nilutamide.

promoter region. The ARE located furthest from the transcriptional start site was designated ARE-1 and that located closest was designated ARE-5. To determine which region(s) in the 5′-flanking region of rOCT2 gene is involved in expressional regulation by testosterone, constructs with deletions of the 5′-flanking region of rOCT2 gene were prepared and their luciferase activities were measured (Fig. 6). On deletion upstream to position −819, there was no induction by testosterone, suggesting that ARE-5 is not involved in the testosterone induction. But, on deletion up to position −1895, testosterone produced a 2-fold increase in activity, indicating that ARE-3 and/or -4 may work as response element(s). Furthermore, as the full-length promoter showed a 3-fold increase in activity, ARE-1 and/or -2 may also function as response elements.

To identify the functional sites for AR's activation, each ARE was mutated. As AR binds to specific response elements organized as an imperfect palindrome sequence (GGTACA nnnTGTTCT), we decided that the 3 bp at position 10–12 were changed to GCC in this sequence because left half-site of ARE is important for androgen receptor and ARE interaction (21). The promoter activity of rOCT2 with a mutation in each ARE revealed that mutated constructs of ARE-1 and ARE-3 were not affected by testosterone (Fig. 7). The other mutated constructs exhibited promoter activity to various extents in response to testosterone. These findings suggested that ARE-1 and ARE-3 play important roles in the activation of the rOCT2 promoter by testosterone.

DISCUSSION

Previously, we and others reported that the expression of rOCT2 mRNA in the kidney differed with gender, but neither rOCT1 nor rOCT3 (11,22), and that exogenous testosterone significantly stimulated only rOCT2 expression in the kidney of both male and female rats (12,23). Serum levels of testosterone were increased to about 1 μM in testosterone-administered rats. In the present study, we demonstrated that rOCT2 promoter activity was stimulated by 1 μM testosterone, whereas rOCT1 and rOCT3 promoters were not (Fig. 2B). These results are consistent with previous *in vivo* findings. 5′-Flanking region about 3000 bp of rOCT2 gene contained five putative AREs. The reporter assay using a series of deletion constructs and mutant constructs for each ARE revealed that ARE-1 (−2975 to −2960) and ARE-3 (−1340 to −1325), which have more similarity to the ARE consensus sequence than any other region, were responsible for the stimulation of rOCT2 promoter activity by testosterone (Figs. 6–7). As the promoter regions of rOCT1 and rOCT3 used in the present study do not have sequences highly homologous to ARE, the absence of an effect by testosterone on these two promoters is reasonable.

It was reported that there was no gender difference in rOCT2 mRNA expression in organs such as the liver and cerebellum (22). This may be a result of the low basal levels of rOCT2 mRNA or of the weak expression of AR in these organs compared to the kidney (24). We previously demonstrated that rOCT2 is predominantly expressed in the kidney, suggesting that some unidentified kidney-specific transcription factors cooperate to stimulate the rOCT2 promoter activity in the presence of testosterone. HEK293 cells (a human embryo kidney cell line) did not show any organic transporter activity (25). When HEK293 cells were used to measure rOCT2 promoter activity in the presence of AR and testosterone, there was no stimulative effect by testosterone (data not shown). It is probable that LLC-PK_1 cells express some transcription factor(s) necessary to express organic cation transporters. Further studies are needed to identify the kidney-specific transcription factors required for rOCT2 expression.

Other transporters have gender differences. For example, the level of rat organic anion transporter 2 (rOAT2) mRNA in the kidney and liver is higher in female than male rats (26,27), and the level of rOAT3 mRNA in male kidney is higher than

Table II. Comparison of the AREs in the Rat OCT2 Promoter Region

Position	Sequence	Homology (%)
ARE consensus	5′-**GGTACAnnnTGTTCT**-3′	–
ARE-1 (−2975 to −2960)	5′-**GGTAGAggaAGCTCT**-3′	80
ARE-3 (−1340 to −1325)	5′-**GGCACAggaTGCTCT**-3′	87
ARE-4 (−1268 to −1253)	5′-**GATACAgacTGTACC**-3′	80
ARE-5 (−548 to −533)	5′-**GAGACTaccTGTTTC**-3′	73

OCT = organic cation transporter.

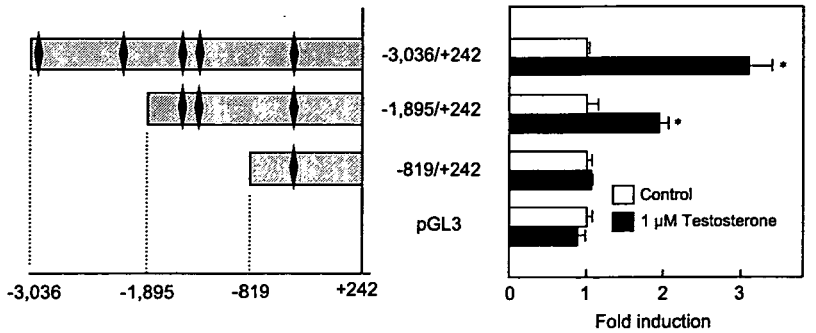

Fig. 6. *Trans*-activation of serial deletions of the rOCT2 promoter by rAR in the presence of testosterone. Various deletion constructs [equimolar amounts of the −3036/+242 construct (0.6 μg)] were transiently transfected into LLC-PK_1 cells with rAR and pRL-TK. The cells were cultured for 43 h with vehicle or 1 μM testosterone, and luciferase activity was measured. Firefly luciferase activity was normalized to *Renilla* luciferase activity. Black diamonds indicate AREs. Each column represents the mean ± SE of three independent experiments. *$p < 0.05$, significantly different from control.

in females (27). Also, gender differences in rat renal cortical OAT1 and OAT3 levels (male > female) are caused by a stimulatory effect of androgens (28). Recently, Ohtsuki *et al.* (29) demonstrated that the expression of OAT3 in rat brain capillary endothelial cells was regulated by testosterone. Although Ohtsuki *et al.* (29) did not carry out reporter assay, it is conceivable that the expressions of the rOAT1 and rOAT3 genes are mediated by the interaction of AR and ARE on these promoters. The present study will be helpful to clarify transcriptional mechanisms of the induction of promoter activities of rOAT1 and rOAT3 by testosterone.

In humans, an evidence is the accumulation of gender differences in the efficacy and toxicity of drugs, and it is thought that physiological factors including body weight, plasma volume, and gastric emptying time are responsible for the variation in drug sensitivity between men and women (30). Recent studies have revealed that other differences, such as cytochrome P450 (CYP), cause gender-related variations in the pharmacokinetics of drugs. It is known that erythromycin (31), nifedipine (32), and verapamil (33), which are metabolized by CYP3A, have greater clearance in women than men. A sex-based difference in the expression of CYP3A4 was detected in the liver (34), but not in the intestine (35). In the renal clearance, amantadine and pramipexole, which are transported by OCT2 (36,37), also exhibit a gender difference (38,39). The renal clearance of amantadine was greater in men than women and was significantly reduced by quinine and quinidine only in men (40). In contrast, the pharmacokinetic parameters of cimetidine and procainamide do not differ between the sexes (41). It is noted that because the luminal efflux may be a rate-limiting step for renal secretion of organic cations (42), large differences in expression of a basolateral human (h)OCT2 may not result in similar large differences in renal clearance. There are some putative AREs in the promoter region of hOCT2, but the positions and sequences are different from those of rOCT2. Further studies are needed to clarify whether the expression of hOCT2 differs with gender, and whether the hOCT2 promoter interacts with the human androgen receptor.

In conclusion, a physiological concentration of testosterone (~10 nM) specifically enhanced transcription of rOCT2 gene, but not of rOCT1 or rOCT3 genes. ARE-1 (−2975 to

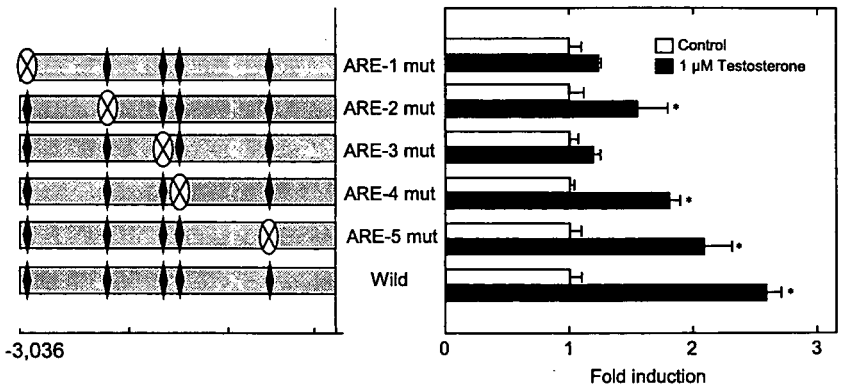

Fig. 7. *Trans*-activation of ARE-mutated rOCT2 promoters by rAR in the presence of testosterone. Constructs were transiently transfected into LLC-PK_1 cells with rAR and pRL-TK. The cells were cultured for 43 h with vehicle or 1 μM testosterone, and luciferase activity was measured. Firefly luciferase activity was normalized to *Renilla* luciferase activity. Black diamonds indicated AREs. Each column represents the mean ± SE of three independent experiments. *$p < 0.05$, significantly different from control.

−2960) and ARE-3 (−1340 to −1325) in the rOCT2 promoter region would play important roles for the enhanced transcription of rOCT2 gene. These findings would account for the transcriptional mechanisms underlying the gender difference in the renal expression of rOCT2 and provide useful information to understand the renal handling of organic cations.

ACKNOWLEDGMENTS

This work was supported in part by the 21st Century COE program "Knowledge Information Infrastructure for Genome Science," a Grant-in-Aid for Scientific Research from the Ministry of Education, Culture, Sports, Science and Technology of Japan, and a Grant-in-Aid for Research on Advanced Medical Technology from the Ministry of Health, Labor and Welfare of Japan. J.A. is supported as a research assistant by the 21st Century COE program "Knowledge Information Infrastructure for Genome Science."

REFERENCES

1. K. Inui and M. Okuda. Cellular and molecular mechanisms of renal tubular secretion of organic anions and cations. *Clin. Exp. Nephrol.* **2**:100–108 (1998).
2. K. Inui, S. Masuda, and H. Saito. Cellular and molecular aspects of drug transport in the kidney. *Kidney Int.* **58**:944–958 (2000).
3. J. W. Jonker and A. H. Schinkel. Pharmacological and physiological functions of the polyspecific organic cation transporters: OCT1, 2, and 3 (SLC22A1–3). *J. Pharmacol. Exp. Ther.* **308**:2–9 (2004).
4. D. Gründemann, V. Gorboulev, S. Gambaryan, M. Veyhl, and H. Koepsell. Drug excretion mediated by a new prototype of polyspecific transporter. *Nature* **372**:549–552 (1994).
5. M. Okuda, H. Saito, Y. Urakami, M. Takano, and K. Inui. cDNA cloning and functional expression of a novel rat kidney organic cation transporter, OCT2. *Biochem. Biophys. Res. Commun.* **224**:500–507 (1996).
6. U. Karbach, J. Kricke, F. Meyer-Wentrup, V. Gorboulev, C. Volk, D. Loffing-Cueni, B. Kaissling, S. Bachmann, and H. Koepsell. Localization of organic cation transporters OCT1 and OCT2 in rat kidney. *Am. J. Physiol. Renal Physiol.* **279**: F679–F687 (2000).
7. M. Sugawara-Yokoo, Y. Urakami, H. Koyama, K. Fujikura, S. Masuda, H. Saito, T. Naruse, K. Inui, and K. Takata. Differential localization of organic cation transporters rOCT1 and rOCT2 in the basolateral membrane of rat kidney proximal tubules. *Histochem. Cell Biol.* **114**:175–180 (2000).
8. R. Kekuda, P. D. Prasad, X. Wu, H. Wang, Y. J. Fei, F. H. Leibach, and V. Ganapathy. Cloning and functional characterization of a potential-sensitive, polyspecific organic cation transporter (OCT3) most abundantly expressed in placenta. *J. Biol. Chem.* **273**:15971–15979 (1998).
9. Y. Urakami, M. Okuda, S. Masuda, M. Akazawa, H. Saito, and K. Inui. Distinct characteristics of organic cation transporters, OCT1 and OCT2, in the basolateral membrane of renal tubules. *Pharm. Res.* **18**:1528–1534 (2001).
10. H. M. Bowman and J. B. Hook. Sex differences in organic ion transport by rat kidney. *Proc. Soc. Exp. Biol. Med.* **141**:258–262 (1972).
11. Y. Urakami, N. Nakamura, K. Takahashi, M. Okuda, H. Saito, Y. Hashimoto, and K. Inui. Gender differences in expression of organic cation transporter OCT2 in rat kidney. *FEBS Lett.* **461**:339–342 (1999).
12. Y. Urakami, M. Okuda, H. Saito, and K. Inui. Hormonal regulation of organic cation transporter OCT2 expression in rat kidney. *FEBS Lett.* **473**:173–176 (2000).
13. H. J. Lee and C. Chang. Recent advances in androgen receptor action. *Cell. Mol. Life Sci.* **60**:1613–1622 (2003).
14. J. A. Tan, K. B. Marschke, K. C. Ho, S. T. Perry, E. M. Wilson, and F. S. French. Response elements of the androgen-regulated C3 gene. *J. Biol. Chem.* **267**:4456–4466 (1992).
15. K. B. Cleutjens, C. C. van Eekelen, H. A. van der Korput, A. O. Brinkmann, and J. Trapman. Two androgen response regions cooperate in steroid hormone regulated activity of the prostate-specific antigen promoter. *J. Biol. Chem.* **271**:6379–6388 (1996).
16. H. Saito, M. Yamamoto, K. Inui, and R. Hori. Transcellular transport of organic cation across monolayers of kidney epithelial cell line LLC-PK. *Am. J. Physiol.* **262**:C59–C66 (1992).
17. Y. Urakami, N. Kimura, M. Okuda, S. Masuda, T. Katsura, and K. Inui. Transcellular transport of creatinine in renal tubular epithelial cell line LLC-PK1. *Drug Metab. Pharmacokinet.* **20**: 200–205 (2005).
18. D. Gründemann J. Babin-Ebell, F. Martel, N. Ording, A. Schmidt, and E. Schömig. Primary structure and functional expression of the apical organic cation transporter from kidney epithelial LLC-PK1 cells. *J. Biol. Chem.* **272**:10408–10413 (2005).
19. J. P. Deslypere, M. Young, J. D. Wilson, and M. J. McPhaul. Testosterone and 5 alpha-dihydrotestosterone interact differently with the androgen receptor to enhance transcription of the MMTV-CAT reporter gene. *Mol. Cell. Endocrinol.* **88**:15–22 (1992).
20. T. Battmann, C. Branche, F. Bouchoux, E. Cerede, D. Philibert, F. Goubet, G. Teutsch, and M. Gaillard-Kelly. Pharmacological profile of RU 58642, a potent systemic antiandrogen for the treatment of androgen-dependent disorders. *J. Steroid Biochem. Mol. Biol.* **64**:103–111 (1998).
21. K. Barbulescu, C. Geserick, I. Schuttke, W. D. Schleuning, and B. Haendler. New androgen response elements in the murine pem promoter mediate selective transactivation. *Mol. Endocrinol.* **15**:1803–1816 (2001).
22. A. L. Slitt, N. J. Cherrington, D. P. Hartley, T. M. Leazer, and C. D. Klaassen. Tissue distribution and renal developmental changes in rat organic cation transporter mRNA levels. *Drug Metab. Dispos.* **30**:212–219 (2002).
23. L. Ji, S. Masuda, H. Saito, and K. Inui. Down-regulation of rat organic cation transporter rOCT2 by 5/6 nephrectomy. *Kidney Int.* **62**:514–524 (2002).
24. H. Takeda, G. Chodak, S. Mutchnik, T. Nakamoto, and C. Chang. Immunohistochemical localization of androgen receptors with mono-and polyclonal antibodies to androgen receptor. *J. Endocrinol.* **126**:17–25 (1990).
25. Y. Urakami, M. Akazawa, H. Saito, M. Okuda, and K. Inui. cDNA cloning, functional characterization, and tissue distribution of an alternatively spliced variant of organic cation transporter hOCT2 predominantly expressed in the human kidney. *J. Am. Soc. Nephrol.* **13**:1703–1710 (2002).
26. Y. Kato, K. Kuge, H. Kusuhara, P. J. Meier, and Y. Sugiyama. Gender difference in the urinary excretion of organic anions in rats. *J. Pharmacol. Exp. Ther.* **302**:483–489 (2002).
27. S. C. Buist, N. J. Cherrington, S. Choudhuri, D. P. Hartley, and C. D. Klaassen. Gender-specific and developmental influences on the expression of rat organic anion transporters. *J. Pharmacol. Exp. Ther.* **301**:145–151 (2002).
28. S. C. Buist, N. J. Cherrington, and C. D. Klaassen. Endocrine regulation of rat organic anion transporters. *Drug Metab. Dispos.* **31**:559–564 (2003).
29. S. Ohtsuki, M. Tomi, T. Hata, Y. Nagai, S. Hori, S. Mori, K. Hosoya, and T. Terasaki. Dominant expression of androgen receptors and their functional regulation of organic anion transporter 3 in rat brain capillary endothelial cells; comparison of gene expression between the blood–brain and –retinal barriers. *J. Cell. Physiol.* **204**:896–900 (2005).
30. J. B. Schwartz. The influence of sex on pharmacokinetics. *Clin. Pharmacokinet.* **42**:107–121 (2003).
31. C. M. Hunt, W. R. Westerkam, and G. M. Stave. Effect of age and gender on the activity of human hepatic CYP3A. *Biochem. Pharmacol.* **44**:275–283 (1992).
32. M. E. Krecic-Shepard, K. Park, C. Barnas, J. Slimko, D. R. Kerwin, and J. B. Schwartz. Race and sex influence clearance of nifedipine: results of a population study. *Clin. Pharmacol. Ther.* **68**:130–142 (2000).
33. K. Dilger, K. Eckhardt, U. Hofmann, K. Kucher, G. Mikus, and M. Eichelbaum. Chronopharmacology of intravenous and oral modified release verapamil. *Br. J. Clin. Pharmacol.* **47**:413–419 (1999).

34. R. Wolbold, K. Klein, O. Burk, A. K. Nussler, P. Neuhaus, M. Eichelbaum, M. Schwab, and U. M. Zanger. Sex is a major determinant of CYP3A4 expression in human liver. *Hepatology* **38**:978–988 (2003).
35. M. F. Paine, S. S. Ludington, M. L. Chen, P. W. Stewart, S. M. Huang, and P. B. Watkins. Do men and women differ in proximal small intestinal CYP3A or P-glycoprotein expression?. *Drug Metab. Dispos.* **33**:426–433 (2005).
36. A. E. Busch, U. Karbach, D. Miska, V. Gorboulev, A. Akhoundova, C. Volk, P. Arndt, J. C. Ulzheimer, M. S. Sonders, C. Baumann, S. Waldegger, F. Lang, and H. Koepsell. Human neurons express the polyspecific cation transporter hOCT2, which translocates monoamine neurotransmitters, amantadine, and memantine. *Mol. Pharmacol.* **54**:342–352 (1998).
37. N. Ishiguro, A. Saito, K. Yokoyama, M. Morikawa, T. Igarashi, and I. Tamai. Transport of the dopamine D2 agonist pramipexole by rat organic cation transporters OCT1 and OCT2 in kidney. *Drug Metab. Dispos.* **33**:495–499 (2005).
38. C. E. Wright, T. L. Sisson, A. K. Ichhpurani, and G. R. Peters. Steady-state pharmacokinetic properties of pramipexole in healthy volunteers. *J. Clin. Pharmacol.* **37**:520–525 (1997).
39. S. E. Gaudry, D. S. Sitar, D. D. Smyth, J. K. McKenzie, and F. Y. Aoki. Gender and age as factors in the inhibition of renal clearance of amantadine by quinine and quinidine. *Clin. Pharmacol. Ther.* **54**:23–27 (1993).
40. L. T. Wong, D. S. Sitar, and F. Y. Aoki. Chronic tobacco smoking and gender as variables affecting amantadine disposition in healthy subjects. *Br. J. Clin. Pharmacol.* **39**:81–84 (1995).
41. M. L. Chen, S. C. Lee, M. J. Ng, D. J. Schuirmann, L. J. Lesko, and R. L. Williams. Pharmacokinetic analysis of bioequivalence trials: implications for sex-related issues in clinical pharmacology and biopharmaceutics. *Clin. Pharmacol. Ther.* **68**:510–521 (2000).
42. S. H. Wright. Role of organic cation transporters in the renal handling of therapeutic agents and xenobiotics. *Toxicol. Appl. Pharmacol.* **204**:309–319 (2005).

BIOCHEMICAL PHARMACOLOGY 71 (2006) 1581–1588

available at www.sciencedirect.com

SCIENCE DIRECT®

journal homepage: www.elsevier.com/locate/biochempharm

The transcription factor Cdx2 regulates the intestine-specific expression of human peptide transporter 1 through functional interaction with Sp1

Jin Shimakura [a], *Tomohiro Terada* [a], *Yutaka Shimada* [b], *Toshiya Katsura* [a], *Ken-ichi Inui* [a,*]

[a] *Department of Pharmacy, Kyoto University Hospital, Faculty of Medicine, Kyoto University, Sakyo-ku, Kyoto 606-8507, Japan*
[b] *Surgery and Surgical Basic Science, Graduate School of Medicine, Kyoto University, Kyoto, Japan*

ARTICLE INFO

Article history:
Received 13 February 2006
Accepted 2 March 2006

Keywords:
PEPT1
Cdx2
Sp1
Transporter
Caco-2
Intestinal metaplasia

Abbreviations:
Cdx2, caudal-related homeobox protein 2
ChIP, chromatin immunoprecipitation
GAPDH, glyceraldehydes-3-phosphate dehydrogenase
HNF, hepatocyte nuclear factor
PEPT1, H+/peptide cotransporter 1
TBS, Tris-buffered saline

ABSTRACT

H^+/peptide cotransporter 1 (PEPT1, SLC15A1) localized at the brush-border membranes of intestinal epithelial cells plays important roles in the intestinal absorption of small peptides and a variety of peptidemimetic drugs. We previously demonstrated that transcription factor Sp1 functions as a basal transcriptional regulator of human PEPT1. However, the factor responsible for the intestine-specific expression of PEPT1 remains unknown. In the present study, we investigated the effect of the intestinal transcription factors on the transcription of the PEPT1 gene and found that only Cdx2 markedly trans-activated the PEPT1 promoter. However, the promoter region responsible for this effect lacked a typical Cdx2-binding sequence, but instead, possessed some Sp1-binding sites. In vitro experiments using Caco-2 cells showed that (1) mutation of the Sp1-binding site diminished the effect of Cdx2, (2) co-expression of Cdx2 and Sp1 synergistically trans-activated the PEPT1 promoter and (3) Sp1 protein was immunoprecipitated with Cdx2 protein. These results raise the possibility that Cdx2 modulates the PEPT1 promoter by interaction with Sp1. The significance of Cdx2 in vivo for PEPT1 regulation was shown by the determination of mRNA levels of Cdx2 and PEPT1 in human tissue. In gastric samples, some with intestinal metaplasia, the levels of PEPT1 and Cdx2 mRNA were highly correlated. Taken together, the present study suggests that Cdx2 plays a key role in the transcriptional regulation of the intestine-specific expression of PEPT1, possibly through interaction with Sp1.

1. Introduction

Di- and tripeptides are taken up into the intestinal and renal epithelial cells by H^+-coupled peptide transporters (PEPT1/SLC15A1 and PEPT2/SLC15A2). Many functional studies using heterologous expression systems have demonstrated molecular natures in their transport characteristics. For example, despite having similar substrate specificity, PEPT1 and PEPT2

* *Corresponding author.* Tel.: +81 75 751 3577; fax: +81 75 751 4207.
E-mail address: inui@kuhp.kyoto-u.ac.jp (K.-i. Inui).
0006-2952/$ – see front matter © 2006 Elsevier Inc. All rights reserved.
doi:10.1016/j.bcp.2006.03.001

were characterized as low- and high-affinity type transporters, respectively [1,2]. In addition, the two transporters differ in their tissue distribution and play distinct physiological roles. PEPT1 is expressed predominantly in the small intestine and slightly in the kidney [1,2]. On the other hand, PEPT2 is expressed mainly in the kidney, but it is also expressed in various tissues such as lung [3], choroid plexus [4] and mammary gland [5], and plays tissue-specific roles. As PEPT1 has broad substrate specificity, the intestinal absorption of several pharmacologically active drugs such as oral β-lactam antibiotics and the anti-viral agent valacyclovir are mediated by this transporter, and therefore, PEPT1 also plays important roles not only as a nutrient transporter but also as a drug transporter [2].

Previously, we isolated the promoter region of PEPT1 and demonstrated that the transcription factor Sp1 plays an important role in the basal transcriptional regulation of PEPT1 [6]. But, as Sp1 is expressed ubiquitously, the intestine-specific expression of PEPT1 cannot be controlled only by Sp1; thus, an intestine-restricted transcription factor is assumed to be involved.

The transcription factor Cdx2 is a member of the caudal-related homeobox gene family and expressed mainly in the intestine [7]. Cdx2 plays important roles in the early differentiation, proliferation and maintenance of intestinal epithelial cells [7,8], and in the transcription of intestinal genes, such as the sucrase–isomaltase [9], lactase–phlorizin hydrolase (LPH) [10], claudin-2 [11] and UDP glucuronosyltransferases genes (UGTs) [12] through binding to a TTTAT/C consensus sequence. Over-expression of Cdx2 in undifferentiated rat IEC-6 intestinal epithelial cells leads to the development of a differentiated phenotype [8]. Furthermore, in humans, CDX2 has been reported to be associated with intestinal metaplasia in the stomach [13] in which ectopic expression of CDX2 is speculated to cause the gastric epithelial cells to trans-differentiate and take the intestinal phenotype. In our recent study, PEPT1 was also found to be expressed in the stomach, induced by intestinal metaplasia [14].

Considering the functions of Cdx2 mentioned above and overlapping of its expression with PEPT1, it is possible to suggest a link between these two genes. In the present study, we investigated the role of Cdx2 in the transcriptional regulation of PEPT1 using the human intestinal cell line Caco-2 cells. In addition, the correlation between PEPT1 and CDX2 mRNA expression levels in human gastric tissue samples developing intestinal metaplasia was also assessed.

2. Materials and methods

2.1. Materials

The anti-CDX2 monoclonal antibody was purchased from BioGenex (San Ramon, CA). The polyclonal antibody recognizing human Sp1 was from Upstate (Charlottesville, VA). The anti-FLAG M2 monoclonal antibody and anti-FLAG M2 monoclonal antibody conjugated to agarose gel (anti-FLAG M2 affinity gel) were obtained from Sigma (St. Louis, MO). The mouse Cdx2 expression vector (pRc/CMV-Cdx2) was a gift from Dr. Eun Ran Suh (University of Pennsylvania). The human HNF-1α and HNF-1β expression vectors were kindly supplied by Dr. Marco Pontoglio (Institute Pasteur, Paris, France). The CMV-Sp1 expression vector was kindly provided by Dr. Robert Tjian (University of California, Berkeley). The FLAG-Cdx2 expression plasmid was constructed by cloning the *Hin*dIII fragment of pRc/CMV-Cdx2 into pFLAG-CMV-6a (Sigma) at the *Hin*dIII restriction site. All other chemicals used were of the highest purity available.

2.2. Cloning of the 5′-regulatory region of PEPT1 gene and preparation of deletion reporter constructs

Cloning of the 5′-regulatory region of the PEPT1 gene and preparation of various reporter constructs were carried out as previously described [6]. Briefly, the 2940-bp flanking region upstream of the transcription start site was subcloned into the firefly luciferase reporter vector, pGL3-Basic (Promega, Madison, WI). This full-length reporter plasmid is hereafter referred to as −2940/+60. The 5′-deleted (−1111/+60, −960/+60, −401/+60, −247/+60, −172/+60 and −21/+60) constructs were generated by digestion of the −2940/+60 construct with the restriction enzymes. The −35/+60 construct was generated by PCR. Site-directed mutations in putative Sp1-binding sites were introduced into the −172/+60 construct with a Quik Change XL site-directed mutagenesis kit (Stratagene, La Jolla, CA).

2.3. Cell culture, transfection and reporter gene assay

Caco-2 cells were obtained from the American Type Culture Collection (ATCC CRL-1392) and maintained in Dulbecco's modified Eagle's medium supplemented with 10% fetal bovine serum and 1% non-essential amino acids. Caco-2 cells were plated into 24-well plates (3×10^5 cells/well) and transfected the following day with the reporter constructs, the expression plasmid for the transcription factor and 2.5 ng of the *Renilla reniformis* vector, pRL-TK (Promega), using Lipofectamine 2000 (Invitrogen Japan KK, Tokyo, Japan) according to the manufacturer's recommendations. The medium was changed after 24 h. The firefly and *Renilla* activities were determined 48 h after the transfection using a dual luciferase assay kit (Promega) and a LB940 luminometer (Berthold, Bad Wildbad, Germany). For the immunoprecipitation and chromatin immunoprecipitation experiments, Caco-2 cells were plated into 60-mm dishes (1.2×10^6 cells/dish) and transfected the following day with the expression plasmid for FLAG-Cdx2 using Lipofectamine 2000.

2.4. Immunoprecipitation and Western blotting

Caco-2 cells expressing FLAG-Cdx2 were washed with PBS twice, scraped off, and suspended in lysis buffer (50 mM Tris–HCl (pH 7.5), 150 mM NaCl, 1% Nonidet P-40, 0.5% sodium deoxycholate, 0.5 mM PMSF and 1% protease inhibitor cocktail (Nacalai tesque, Kyoto, Japan)). After an incubation at 4 °C for 15 min, the cells were disrupted by vigorous vortexing and repeated passages through a 24-gauge needle. The homogenate was centrifuged at 4 °C and 20,000 ×*g* for 10 min, and the supernatant was recovered. Immunoprecipitation of FLAG-Cdx2 was performed using anti-FLAG affinity gel at 4 °C overnight. The gel was washed with the lysis buffer five times. The immunoprecipitated FLAG-Cdx2 proteins were solubilized

in SDS sample buffer, separated on a 10% polyacrylamide gel at room temperature, and transferred onto polyvinylidene difluoride membranes (Immobilon-P; Millipore, Bedford, MA) by semidry electroblotting. Blots were blocked with 5% nonfat dry milk in Tris-buffered saline (TBS; 20 mM Tris, 137 mM NaCl, pH 7.5) with 0.1% Tween 20 (TBS-T) for 3 h at room temperature. The blots were washed in TBS-T and then incubated with the anti-FLAG M2 monoclonal antibody (10 μg/ml, 1 h at room temperature) or anti-Sp1 polyclonal antibody (1 μg/ml, overnight at 4 °C). Blots were washed three times with TBS-T, and the bound antibody was detected on X-ray film by enhanced chemiluminescence with a horseradish peroxidase-conjugated anti-mouse or anti-rabbit IgG antibody (Amersham Pharmacia Biotech, Piscataway, NJ).

2.5. Chromatin immunoprecipitation (ChIP)

Caco-2 cells expressing FLAG-Cdx2 were cross-linked with 1% formaldehyde at room temperature for 10 min. Cells then were rinsed with ice-cold PBS twice, scraped off, and suspended in lysis buffer (50 mM Tris–HCl (pH 7.5), 150 mM NaCl, 1% Nonidet P-40, 0.5% sodium deoxycholate, 0.5 mM PMSF and 1% protease inhibitor cocktail). Cells were sonicated three times for 15 s each time at 40% of the maximal setting (VP-5S, TAITEC, Koshigaya, Japan) and centrifuged at 4 °C and 20,000 ×*g* for 10 min. After the supernatants were collected and diluted in lysis buffer, immunoprecipitation was performed overnight at 4 °C with anti-FLAG affinity gel. The gel was then washed five times with lysis buffer and extracted with 1.5% SDS, followed by 0.5% SDS. Eluates were pooled and heated at 68 °C for 6 h to reverse the formaldehyde cross-linking. Chromatin-associated proteins were digested with proteinase K at 55 °C. The DNA was recovered by phenol–chloroform extraction and ethanol precipitation. Pellets were dissolved in 20 μl of TE buffer and used as a template for PCR. Primers used for amplifying the PEPT1 promoter were 5′-GACTGGCTCTCCCCCGGCCTGCCACG-3′ and 5′-CCCGGCCCCGTTGCCCCAGGTACAGC-3′ (−209 to −26 upstream of the transcriptional start site). PCR was performed using Advantage GC Genomic Polymerase Mix (BD Biosciences, Franklin Lakes, NJ) and cycling conditions were as follows: 1 min of denaturation at 95 °C, followed by 30 cycles of 30 s of denaturation at 94 °C, 3 min of primer annealing and extension at 68 °C, and 3 min of final extension at 68 °C.

2.6. Human gastric tissue sample

The gastric mucosal samples from normal stomachs were obtained from cancer patients ($n = 30$) during surgery at the First Department of Surgery, Kyoto University Hospital. Normal mucosal samples were resected at the site most distant from the affected portions. Three samples from different portions were resected in some patients. Pathologists diagnosed intestinal metaplasia in some patients. No patients underwent preoperative chemotherapy and/or radiation therapy. The samples were frozen in liquid nitrogen and stored at −80 °C until RNA extraction. This study was conducted in accordance with the Declaration of Helsinki and its amendments, and was approved by the Ethics Committee of Kyoto University (G-39). Written informed consent was obtained from all patients for surgery and the use of their resected samples.

2.7. Real-time PCR

Isolation of total RNA from the human stomach samples and real-time PCR were carried out as described previously [14]. The primer–probe set used for CDX2 was pre-developed TaqMan Assay Reagents (Applied Biosystems, Foster, CA). Glyceraldehydes-3-phosphate dehydrogenase (GAPDH) mRNA was also measured as an internal control with GAPDH Control Reagent (Applied Biosystems).

2.8. Data analysis

The results were expressed relative to the result obtained with the pGL3-Basic vector set as 1 and represent the means ± S.E. ($n = 3$). Two or three experiments were conducted, and representative results were shown. In the mutational experiment, statistical analysis was performed with the one-way ANOVA followed by Scheffé F post hoc testing.

3. Results

3.1. Cdx2 activates transcription of the PEPT1 promoter-reporter construct

To investigate whether Cdx2 activates the PEPT1 promoter, the −2940/+60 reporter construct was transiently transfected into Caco-2 cells simultaneously with Cdx2 expression plasmids. Besides Cdx2, the transcription factor hepatocyte nuclear factor (HNF)-1α is also expressed in the intestine and involved in the expression of some intestinal genes although it was first discovered in the liver [15,16]. In the regulation of LPH expression, Cdx2 is reported to directly interact with HNF-1α [10]. Thus, the effect of HNF-1α and a related transcription factor, HNF-1β, on the PEPT1 promoter was also assessed. Cdx2 over-expression resulted in a four-fold increase in promoter activity (Fig. 1). However, HNF-1α could neither activate the PEPT1 promoter nor enhance its activity driven by Cdx2. HNF-1β could activate it only a little as compared to Cdx2. Thus, we focused on Cdx2 as a possible regulator of PEPT1 expression and further investigated the Cdx2-responsive region in the PEPT1 promoter.

3.2. Cdx2-responsive region located near the Sp1-binding sites

To determine the elements contributing to the expression of PEPT1, we carried out a promoter 5′-deletion analysis (Fig. 2). The promoter activity in the absence of Cdx2 was strongest with the −401/+60 construct and gradually decreased by the deletion between −401 and −35, consistent with our previous result [6]. The promoter activity in the presence of Cdx2 increased three- to four-fold as compared to that in the absence of Cdx2 with the −2940 to −172 constructs whereas it was completely diminished with the −35/+60 construct, suggesting that the Cdx2-responsive region is located between −172 and −35. Unexpectedly, this region lacked a consensus Cdx2-binding site but contained multiple Sp1-binding sites as reported previously [6]. We could not find any transcription factor-binding sites which are likely to be responsible for the

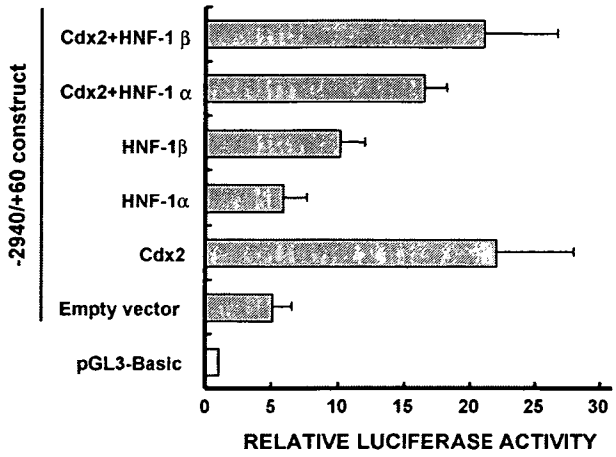

Fig. 1 – Effects of Cdx2, HNF-1α and HNF-1β overexpression on the PEPT1 promoter activity. Caco-2 cells were transiently transfected with 250 ng of the −2940/+60 construct and 250 ng of the expression vector for Cdx2, HNF-1α or HNF-1β. The total amount of transfected DNA (750 ng) was kept constant by adding empty vector. Firefly luciferase activity was normalized to *Renilla* luciferase activity. Data are reported as the relative fold-increase compared with pGL3-Basic and represent the mean ± S.E. ($n = 3$).

effect of Cdx2 except for Sp1 in this region. We next carried out a mutational analysis to determine whether the effect of Cdx2 was mediated through these Sp1-binding sites. The promoter activity in the absence of Cdx2 was reduced with the mutation of Sp-A, Sp-B or Sp-C sites, consistent with our prior study [6]. Trans-activation by Cdx2 was markedly decreased with the construct possessing the mutation of Sp-A or Sp-C sites (Fig. 3). These deletion and mutational analyses collectively suggest that Cdx2 may functions via interaction with Sp1 on the PEPT1 promoter.

3.3. *PEPT1 promoter was synergistically activated by Cdx2 and Sp1*

Sp1 has been shown to trans-activate the PEPT1 promoter [6]. We therefore determined whether Cdx2 enhances the promoter activity in cooperation with Sp1. Cdx2 or Sp1 alone caused a 1.5–2-fold increase of the promoter activity, whereas co-expression of Cdx2 and Sp1 resulted in a four-fold increase in the promoter activity (Fig. 4), suggesting a synergistic effect.

3.4. *Protein–protein interaction of Cdx2 and Sp1*

The synergistic effect of Cdx2 and Sp1 observed in the co-expression experiment, together with the observations from the mutational analysis, raise the possibility that these two proteins interact physically to regulate PEPT1 expression. We therefore investigated the interaction of Cdx2 and Sp1 within the cell using co-immunoprecipitation. Whole-cell extracts of Caco-2 cells transfected with the expression vector for FLAG-Cdx2 or empty vector were subjected to immunoprecipitation followed by Western blotting. Detection with anti-FLAG antibody confirmed that FLAG-Cdx2 protein was expressed in the cells transfected with FLAG-Cdx2 and appropriately immunoprecipitated (Fig. 5, upper panel). In the input samples, as expected, the band of Sp1 protein was detected both in the cells transfected with FLAG-Cdx2 and empty vector, while in the immunoprecipitated sample, it was detected only in the FLAG-Cdx2 transfected cells (Fig. 5, lower panel). These findings show that endogenous Sp1 protein was co-immunoprecipitated with FLAG-Cdx2 and suggest that Cdx2 and Sp1 were associated in a protein complex in Caco-2 cells.

3.5. *Cdx2 associates with the PEPT1 promoter*

As mentioned above, the Cdx2-responsive region lacked a consensus Cdx2-binding site, and an electrophoretic mobility shift assay failed to demonstrate the binding of Cdx2 with the PEPT1 promoter (data not shown). Thus we adopted an

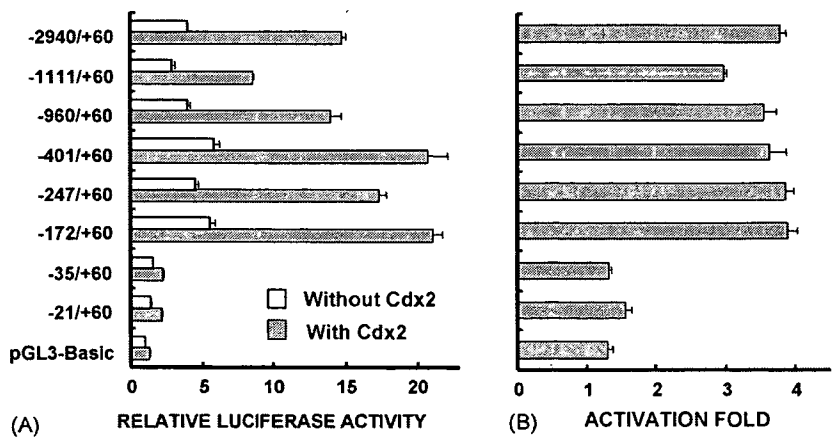

Fig. 2 – Identification of the Cdx2-responsive region in the PEPT1 promoter. A series of deleted promoter constructs (equimolar amounts of the −2940/+60 construct (500 ng)) and 500 ng of the Cdx2 expression vector or empty vector were transiently transfected into Caco-2 cells for luciferase assays. Firefly luciferase activity was normalized to *Renilla* luciferase activity. Data are reported as the relative fold-increase compared with the pGL3-Basic vector (A) or as the ratio of Cdx2-expressing vector to empty vector (B) and represent the mean ± S.E. ($n = 3$).

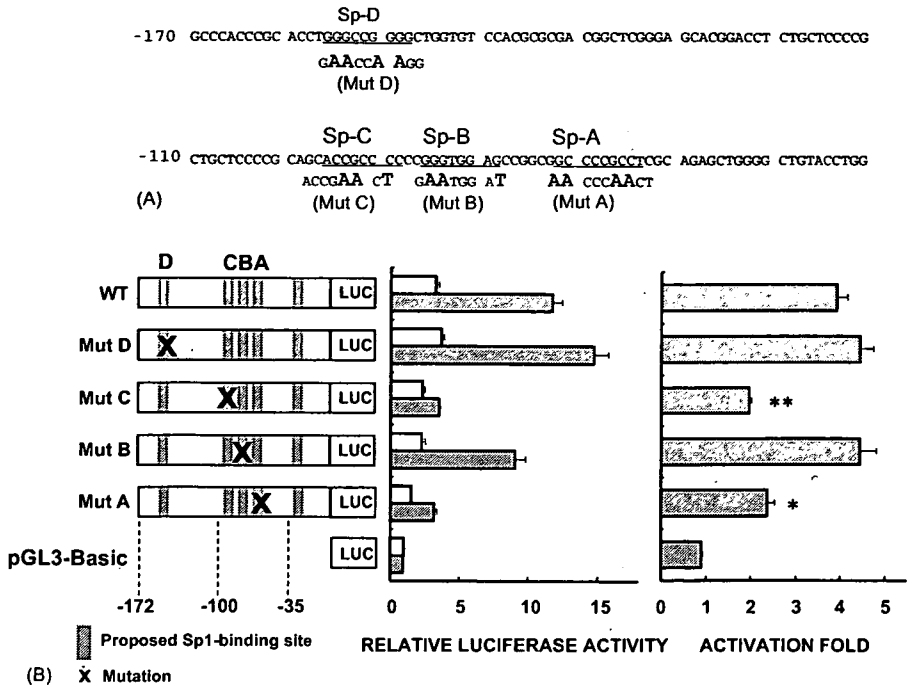

Fig. 3 – Mutational analysis of Sp1-binding sites in the Cdx2-responsive region in the PEPT1 promoter. (A) The nucleotide sequence of the promoter region from −170 to −41 is shown with the putative Sp1-binding elements (Sp-A, Sp-B, Sp-C, Sp-D, underlined). Site-directed mutations that destroy Sp1-binding elements were introduced individually and designated mut A, mut B, mut C and mut D. The nucleotides altered for mutational analysis are shown in bold letters under the wild-type sequence. (B) The mutated −172/+60 constructs (500 ng) and 500 ng of the Cdx2 expression vector or empty vector were transiently expressed in Caco-2 cells for luciferase assays. Firefly luciferase activity was normalized to *Renilla* luciferase activity. Data are reported as the relative fold-increase compared with the pGL3-Basic vector and as the ratio of Cdx2-expressing vector to empty vector, and represent the mean ± S.E. ($n = 3$). (* and **) Significantly different from wild type (WT), $^{*}p < 0.05$, $^{**}p < 0.01$.

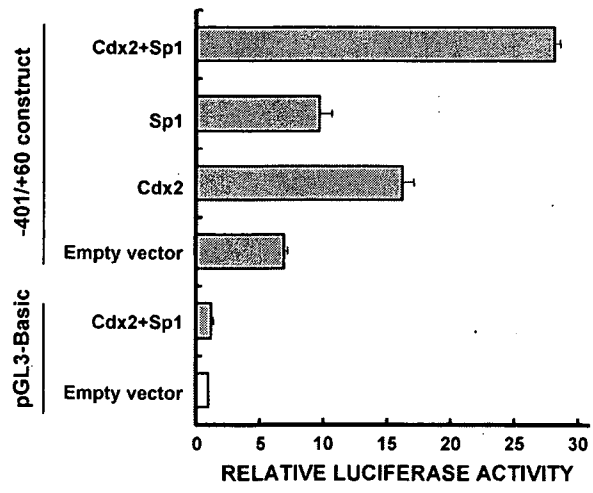

Fig. 4 – Synergistic activation of the PEPT1 promoter by Cdx2 and Sp1. Caco-2 cells were transiently transfected with 150 ng of the −401/+60 construct and the expression vector for Cdx2 (500 ng) or Sp1 (1000 ng). The total amount of transfected DNA (1650 ng) was kept constant by adding empty vectors. Data are reported as the relative fold-increase compared with pGL3-Basic and represent the mean ± S.E. ($n = 3$).

alternative methodology, the ChIP assay, to investigate the association of Cdx2 with the PEPT1 promoter. An approximately 200-bp fragment of the PEPT1 promoter covering the Cdx2-responsive region, which had the Sp1-binding sites, was recovered by immunoprecipitation of FLAG-Cdx2 from the transfected cells, whereas only a trace amount of the fragment was recovered from the mock-transfected cells (Fig. 6).

3.6. *The level of PEPT1 mRNA is correlated with that of CDX2 in the gastric samples with the intestinal metaplasia*

mRNA levels of PEPT1 and CDX2 in the human gastric samples, some with intestinal metaplasia, were determined using quantitative real-time PCR (Fig. 7). PEPT1 and CDX2 mRNA levels differed by more than 100-fold between the samples. The mRNA level of PEPT1 was highly correlated with that of CDX2. Furthermore, both PEPT1 and CDX2 were expressed at apparently higher levels in the samples diagnosed pathologically with intestinal metaplasia as compared to the normal tissue.

4. Discussion

The molecular mechanisms responsible for the intestine-specific expression of PEPT1 are largely unknown. In the

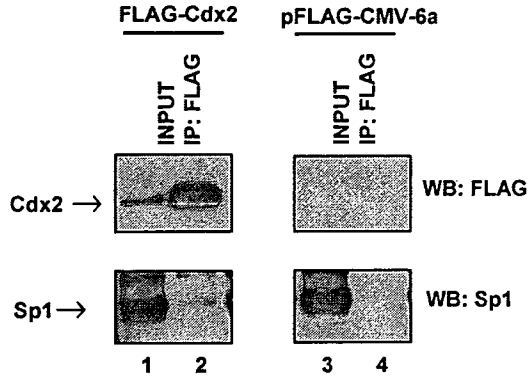

Fig. 5 – Physical interaction of Cdx2 with Sp1 protein. Whole-cell extracts of Caco-2 cells transfected with FLAG-Cdx2 or pFLAG-CMV-6a (empty vector) were subjected to immunoprecipitation followed by Western blotting. Proteins were immunoprecipitated with anti-FLAG M2 affinity gel (lanes 2 and 4, indicated as IP:FLAG). Whole-cell extracts before immunoprecipitation were also analyzed (lanes 1 and 3, indicated as INPUT). FLAG-Cdx2 and Sp1 protein were detected with anti-FLAG M2 monoclonal antibody (upper panels) and anti-Sp1 polyclonal antibody (lower panels), respectively.

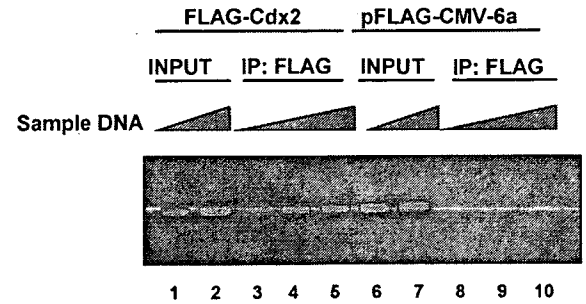

Fig. 6 – Association of Cdx2 with the PEPT1 promoter. Chromatin immunoprecipitation analysis of the endogenous PEPT1 promoter in Caco-2 cells transfected with FLAG-Cdx2 or pFLAG-CMV-6a (empty vector) was performed. The immunoprecipitated DNA fragments were purified and amplified by PCR with primers spanning the Cdx2-responsive region, and subjected to agarose gel electrophoresis. Serially diluted samples of DNA were used for PCR amplification. Lanes 1, 2 and 6, 7 indicate INPUT DNA. Lanes 3–5 and 8–10 show immunoprecipitated DNA.

present study, we provide the first evidence that Cdx2 regulates the transcription of PEPT1 using Caco-2 cells. Unlike other intestinal genes, such as the genes for LPH [10], claudin-2 [11] and UGTs [12], neither HNF-1α nor HNF-1β could trans-activate the PEPT1 promoter, although Cdx2 markedly enhanced the activity of the PEPT1 promoter. Deletion analysis revealed that the Cdx2-responsive region was located between bases −172 and −35 relative to the transcription start site. Computational analysis showed the lack of a canonical Cdx2-binding site in this region, but the presence of several GC-boxes which we previously identified as Sp1-binding sites. Sp1 has been reported to interact with various transcription factors or co-factors, such as estrogen receptor [17], p300/CREB-binding protein [18] and homeobox protein, Hox proteins [19]. Thus we tried to elucidate whether Cdx2 interacts with Sp1 to regulate the PEPT1 promoter.

Introducing mutations into Sp1-binding sites reduced the effect of Cdx2. Furthermore, co-expression of Cdx2 and Sp1 synergistically activated the PEPT promoter. These results suggest that the trans-activating effect of Cdx2 might be mediated via a Sp1-dependent mechanism. Among Sp1-binding sites located in Cdx2-responsive region, Sp-A, Sp-B and Sp-C were involved in the basal promoter activity, whereas only Sp-A and Sp-C appeared to be critical for Cdx2 effect, indicating that the regulatory effect of Cdx2 is site-dependent.

Co-immunoprecipitation of FLAG-tagged Cdx2 precipitated the endogenous Sp1 protein, suggesting the formation of a transcriptional complex involving Cdx2 and Sp1. In addition, ChIP assays indicated that Cdx2 protein was present on the

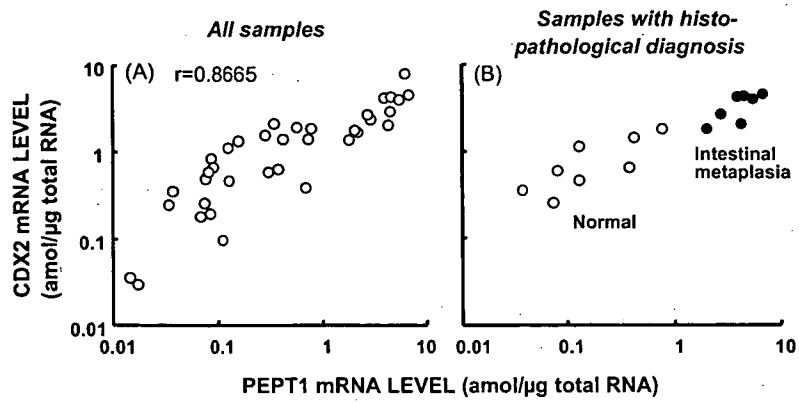

Fig. 7 – Correlation between PEPT1 and CDX2 mRNA levels in the human gastric tissue samples. The mRNA levels of PEPT1 and CDX2 were quantified with real-time PCR analysis in the gastric mucosal samples. Some of these tissue samples were diagnosed by a pathologist and proved to be intestinal metaplasia. (A) All samples were plotted. (B) The samples of patients diagnosed by a pathologist were plotted. Open and closed symbols indicate the normal samples and the samples proved to be intestinal metaplasia, respectively.

PEPT1 promoter at the whole cell level. Considering the lack of Cdx2-binding site in the Cdx2-responsive region and the functional and physical interaction between Cdx2 and Sp1 mentioned above, one explanation for the regulatory mechanism of Cdx2 may be that Cdx2 protein associates with the PEPT1 promoter via the complex formation with Sp1. Although Cdx2 has been reported to interact with the transcription factors such as HNF-1α [10–12] and GATA proteins [20], in all cases, Cdx2 directly binds to its cognate binding site on the promoter of target genes. By contrast, Cdx2 is speculated to exert its effect without direct binding to its cognate binding sequence on the PEPT1 promoter. The nature of the physical interaction between Cdx2 and Sp1 has yet to be determined. One possibility is that Cdx2 directly binds to Sp1 protein. Another possibility is indirect binding mediated by a common cofactor or some adaptor proteins. In both cases, to our knowledge, this is a novel mechanism of transcriptional regulation by Cdx2. Further studies will be needed to obtain the additional proof for supporting and fully characterizing this proposed mechanism.

In order to demonstrate the significance of Cdx2 for PEPT1 expression in vivo, we next investigated the expression profile of Cdx2 and PEPT1 mRNA using human tissue samples. In the gastric samples, some of which had intestinal metaplasia, PEPT1 and Cdx2 mRNA levels were highly correlated. The fact that ectopic expression of Cdx2 accompanied the expression of PEPT1 in human tissues strongly supports the role of Cdx2 demonstrated by in vitro reporter experiments. In addition, a recent study showed that expression of PEPT1 was induced in the gastric epithelium in a transgenic mouse expressing Cdx2 exclusively in the gastric epithelium [21].

The similarities between PEPT1 and Cdx2 in their expression profile are observed not only at the tissue level but also at the cellular level. PEPT1 is localized to brush-border membranes of the absorptive epithelial cells of the small intestine, and this protein is abundant at the tip of the villus and scarce at the crypt base [22]. Cdx2 also has a gradient of expression in the crypt–villus axis being primarily expressed in the villus [7].

It has been reported that intestinal PEPT1 is regulated by various factors [23], such as thyroid hormone [24], dietary conditions [25,26], diurnal rhythm [27] and a selective σ-ligand, pentazocine [28]. In addition, the ectopic induction of PEPT1 expression in the colon, where PEPT1 was not expressed under normal conditions, was observed in cases of functional deficiency of the small intestine such as ulcerative colitis, Crohn's disease and short-bowel syndrome [23]. It is not clear at present whether Cdx2 plays some parts in these regulatory functions. However, Cdx2 exerts physiological roles in the differentiation of intestinal epithelial cells and maintenance of intestinal phenotype. It is possible that Cdx2 helps to regulate colonic PEPT1 expression under such pathological conditions.

In conclusion, we demonstrated that Cdx2 regulated the PEPT1 promoter activity in Caco-2 cells using reporter assays, and confirmed the significance of Cdx2 in vivo in a correlation analysis of mRNA expression in human tissue samples. In addition, it may be possible that Cdx2 physically and functionally interacts with Sp1, and associates with the PEPT1 promoter although no cognate Cdx2-binding site is evident. These results collectively indicate that Cdx2 plays a key role in the transcriptional regulation for the intestine-specific expression of PEPT1, and have implications as a basis for future investigations of efficient enteral nutrition and drug therapy.

Acknowledgments

We are grateful to Dr. Eun Ran Suh (University of Pennsylvania) and Dr. Robert Tjian (University of California, Berkeley) for the generous gift of Cdx2 and Sp1 expression vectors, respectively. We also thank Dr. Marco Pontoglio (Institute Pasteur, Paris, France) for kindly providing Human HNF-1α and HNF-1β expression vectors.

This work was supported by the 21st Century COE Program "Knowledge Information Infrastructure for Genome Science", a Grant-in-Aid for Scientific Research from the Ministry of Education, Culture and Sports of Japan, and a Grant-in-Aid for Research on Advanced Medical Technology from the Ministry of Health, Labor and Welfare of Japan.

REFERENCES

[1] Daniel H. Molecular and integrative physiology of intestinal peptide transport. Annu Rev Physiol 2004;66:361–84.
[2] Terada T, Inui K. Peptide transporters: structure, function, regulation and application for drug delivery. Curr Drug Metabol 2004;5:85–94.
[3] Groneberg DA, Nickolaus M, Springer J, Doring F, Daniel H, Fischer A. Localization of the peptide transporter PEPT2 in the lung: implications for pulmonary oligopeptide uptake. Am J Pathol 2001;158:707–14.
[4] Berger UV, Hediger MA. Distribution of peptide transporter PEPT2 mRNA in the rat nervous system. Anat Embryol 1999;199:439–49.
[5] Groneberg DA, Doring F, Theis S, Nickolaus M, Fischer A, Daniel H. Peptide transport in the mammary gland: expression and distribution of PEPT2 mRNA and protein. Am J Physiol Endocrinol Metab 2002;282:E1172–9.
[6] Shimakura J, Terada T, Katsura T, Inui K. Characterization of the human peptide transporter PEPT1 promoter: Sp1 functions as a basal transcriptional regulator of human PEPT1. Am J Physiol Gastrointest Liver Physiol 2005;289:G471–7.
[7] Silberg DG, Swain GP, Suh ER, Traber PG. Cdx1 and Cdx2 expression during intestinal development. Gastroenterology 2000;119:961–71.
[8] Suh E, Traber PG. An intestine-specific homeobox gene regulates proliferation and differentiation. Mol Cell Biol 1996;16:619–25.
[9] Suh E, Chen L, Taylor J, Traber PG. A homeodomain protein related to caudal regulates intestine-specific gene transcription. Mol Cell Biol 1994;14:7340–51.
[10] Mitchelmore C, Troelsen JT, Spodsberg N, Sjostrom H, Noren O. Interaction between the homeodomain proteins Cdx2 and HNF1alpha mediates expression of the lactase-phlorizin hydrolase gene. Biochem J 2000;346:529–35.
[11] Sakaguchi T, Gu X, Golden HM, Suh E, Rhoads DB, Reinecker HC. Cloning of the human claudin-2 5′-flanking region revealed a TATA-less promoter with conserved binding sites in mouse and human for caudal-related homeodomain proteins and hepatocyte nuclear factor-1alpha. J Biol Chem 2002;277:21361–70.
[12] Gregory PA, Lewinsky RH, Gardner-Stephen DA, Mackenzie PI. Coordinate regulation of the human UDP

glucuronosyltransferase 1A8, 1A9, and 1A10 genes by hepatocyte nuclear factor 1α and the caudal-related homeodomain protein 2. Mol Pharmacol 2004;65:953–63.
[13] Almeida R, Silva E, Santos-Silva F, Silberg DG, Wang J, De Bolos C, et al. Expression of intestinespecific transcription factors, CDX1 and CDX2, in intestinal metaplasia and gastric carcinomas. J Pathol 2003;199:36–40.
[14] Terada T, Shimada Y, Pan X, Kishimoto K, Sakurai T, Doi R, et al. Expression profiles of various transporters for oligopeptides, amino acids and organic ions along the human digestive tract. Biochem Pharmacol 2005;70: 1756–63.
[15] Baumhueter S, Mendel DB, Conley PB, Kuo CJ, Turk C, Graves MK, et al. HNF-1 shares three sequence motifs with the POU domain proteins and is identical to LF-B1 and APF. Genes Dev 1990;4:372–9.
[16] Mendel DB, Crabtree GR. HNF-1, a member of a novel class of dimerizing homeodomain proteins. J Biol Chem 1991;266:677–80.
[17] Sun JM, Spencer VA, Li L, Yu Chen H, Yu J, Davie JR. Estrogen regulation of trefoil factor 1 expression by estrogen receptor α and Sp proteins. Exp Cell Res 2005;302:96–107.
[18] Jang SI, Steinert PM. Loricrin expression in cultured human keratinocytes is controlled by a complex interplay between transcription factors of the Sp1, CREB, AP1, and AP2 families. J Biol Chem 2002;277:42268–79.
[19] Suzuki M, Ueno N, Kuroiwa A. Hox proteins functionally cooperate with the GC box-binding protein system through distinct domains. J Biol Chem 2003;278:30148–56.
[20] Boudreau F, Rings EH, van Wering HM, Kim RK, Swain GP, Krasinski SD, et al. Hepatocyte nuclear factor-1 alpha, GATA-4, and caudal related homeodomain protein Cdx2 interact functionally to modulate intestinal gene transcription. Implication for the developmental regulation of the sucrase-isomaltase gene. J Biol Chem 2002;277:31909–17.
[21] Mutoh H, Satoh K, Kita H, Sakamoto H, Hayakawa H, Yamamoto H, et al. Cdx2 specifies the differentiation of morphological as well as functional absorptive enterocytes of the small intestine. Int J Dev Biol 2005;49:867–71.
[22] Ogihara H, Saito H, Shin BC, Terada T, Takenoshita S, Nagamachi Y, et al. Immuno-localization of H+/peptide cotransporter in rat digestive tract. Biochem Biophys Res Commun 1996;220:848–52.
[23] Adibi SA. Regulation of expression of the intestinal oligopeptide transporter (Pept-1) in health and disease. Am J Physiol Gastrointest Liver Physiol 2003;285:G779–88.
[24] Ashida K, Katsura T, Motohashi H, Saito H, Inui K. Thyroid hormone regulates the activity and expression of the peptide transporter PEPT1 in Caco-2 cells. Am J Physiol Gastrointest Liver Physiol 2002;282:G617–23.
[25] Naruhashi K, Sai Y, Tamai I, Suzuki N, Tsuji A. Pept1 mRNA expression is induced by starvation and its level correlates with absorptive transport of cefadroxil longitudinally in the rat intestine. Pharm Res 2002;19:1417–23.
[26] Shiraga T, Miyamoto K, Tanaka H, Yamamoto H, Taketani Y, Morita K, et al. Cellular and molecular mechanisms of dietary regulation on rat intestinal H^+/peptide transporter PepT1. Gastroenterology 1999;116:354–62.
[27] Pan X, Terada T, Irie M, Saito H, Inui K. Diurnal rhythm of H^+-peptide cotransporter in the rat small intestine. Am J Physiol Gastrointest Liver Physiol 2002;283:G57–64.
[28] Fujita T, Majikawa Y, Umehisa S, Okada N, Yamamoto A, Ganapathy V, et al. σ-Receptor ligand-induced up-regulation of the H^+/peptide transporter PEPT1 in the human intestinal cell line Caco-2. Biochem Biophys Res Commun 1999;261:242–6.

0022-3565/06/3181-455–460$20.00
THE JOURNAL OF PHARMACOLOGY AND EXPERIMENTAL THERAPEUTICS
Copyright © 2006 by The American Society for Pharmacology and Experimental Therapeutics
JPET 318:455–460, 2006

Vol. 318, No. 1
102830/3120199
Printed in U.S.A.

Transport Characteristics of a Novel Peptide Transporter 1 Substrate, Antihypotensive Drug Midodrine, and Its Amino Acid Derivatives

Masahiro Tsuda, Tomohiro Terada, Megumi Irie, Toshiya Katsura, Ayumu Niida, Kenji Tomita, Nobutaka Fujii, and Ken-ichi Inui

Department of Pharmacy, Kyoto University Hospital, Faculty of Medicine (M.T., T.T., M.I., T.K., K.I.), and Graduate School of Pharmaceutical Science (A.N., K.T., N.F.), Kyoto University, Kyoto, Japan

Received February 12, 2006; accepted April 4, 2006

ABSTRACT

Midodrine is an oral drug for orthostatic hypotension. This drug is almost completely absorbed after oral administration and converted into its active form, 1-(2′,5′-dimethoxyphenyl)-2-aminoethanol) (DMAE), by the cleavage of a glycine residue. The intestinal H^+-coupled peptide transporter 1 (PEPT1) transports various peptide-like drugs and has been used as a target molecule for improving the intestinal absorption of poorly absorbed drugs through amino acid modifications. Because midodrine meets these requirements, we examined whether midodrine can be a substrate for PEPT1. The uptake of midodrine, but not DMAE, was markedly increased in PEPT1-expressing oocytes compared with water-injected oocytes. Midodrine uptake by Caco-2 cells was saturable and was inhibited by various PEPT1 substrates. Midodrine absorption from the rat intestine was very rapid and was significantly inhibited by the high-affinity PEPT1 substrate cyclacillin, assessed by the alteration of the area under the blood concentration-time curve for 30 min and the maximal concentration. Some amino acid derivatives of DMAE were transported by PEPT1, and their transport was dependent on the amino acids modified. In contrast to neutral substrates, cationic midodrine was taken up extensively at alkaline pH, and this pH profile was reproduced by a 14-state model of PEPT1, which we recently reported. These findings indicate that PEPT1 can transport midodrine and contributes to the high bioavailability of this drug and that Gly modification of DMAE is desirable for a prodrug of DMAE.

H^+-coupled peptide transporter 1 (PEPT1) expressed in the brush-border membranes of intestinal epithelial cells transports dipeptides and tripeptides from the lumen into cells using an inward H^+-electrochemical gradient (Inui and Terada, 1999; Daniel, 2004; Terada and Inui, 2004). In addition to dipeptides and tripeptides, various peptide-like drugs, such as oral β-lactam antibiotics, can be transported by PEPT1; therefore, PEPT1 serves as a drug transporter (Yang et al., 1999; Daniel and Kottra, 2004; Terada and Inui, 2004). Over the last decade, PEPT1 has been used as a target molecule for improving the intestinal absorption of poorly absorbed drugs through amino acid modifications. For example, the enhanced oral bioavailability of valacyclovir and valganciclovir, amino acid ester prodrugs of acyclovir and ganciclovir, respectively, has been attributed to their enhanced intestinal transport via PEPT1 (Han et al., 1998; Sugawara et al., 2000).

Midodrine is a selective α1-receptor agonist to treat orthostatic hypotension and is a prodrug of 1-(2′,5′-dimethoxyphenyl)-2-aminoethanol (DMAE) to combine the glycine by a peptide bond. After oral administration, the bioavailability of midodrine is reported to be approximately 100%, whereas that of DMAE is approximately 50%. However, mechanisms of improving intestinal absorption of midodrine have not been elucidated.

Midodrine resembles a dipeptide in structure, and improving the intestinal absorption of DMAE by modifying an amino acid is similar to the relationship between acyclovir and valacyclovir. Based on this background, in the present study, we examined whether midodrine can be a substrate for PEPT1 in vitro and in vivo. Furthermore, we synthesized various DMAE amino acid derivatives to clarify which amino

This work was supported by the 21st Century Center of Excellence Program "Knowledge Information Infrastructure for Genome Science," the Leading Project for Biosimulation, a grant-in-aid for Scientific Research from the Ministry of Education, Culture and Sports of Japan, and a grant-in-aid for Research on Advanced Medical Technology from the Ministry of Health, Labor and Welfare of Japan.

Article, publication date, and citation information can be found at http://jpet.aspetjournals.org.

doi:10.1124/jpet.106.102830.

ABBREVIATIONS: PEPT1, H^+-coupled peptide transporter 1; DMAE, 1-(2′,5′-dimethoxyphenyl)-2-aminoethanol; MES, 2-(*N*-morpholino)ethanesulfonic acid; HPLC, high-performance liquid chromatography; TFA, trifluoroacetic acid; AUC, area under the curve.

acid modification by a peptide bond is the most suitable for interaction with PEPT1 using DMAE as a model compound. We do not have enough information regarding this issue, although there are various reports to examine the interaction of amino acid esterification of poorly absorbed drugs with PEPT1 (Han et al., 1998; Sawada et al., 1999). Finally, we simulated pH profiles of midodrine (cationic) and a glutamate derivative of DMAE (neutral) using a 14-state model of PEPT1, which we constructed recently (Irie et al., 2005).

Materials and Methods

Materials. Midodrine and DMAE were gifts from Taisho Pharmaceutical (Tokyo, Japan). [^{3}H]Glycylsarcosine (4 Ci/mmol) was obtained from Moravek Biochemicals Inc. (Brea, CA). Glycylsarcosine was purchased from Sigma Chemical Co. (St. Louis, MO). All other chemicals used were of the highest purity available.

DMAE Amino Acid Derivatives Synthesis. Figure 1 shows the structures of DMAE amino acid derivatives. The derivatives were obtained as follows. Diisopropylethylamine (1 Eq), *N*-Boc-protected amino acid (1 Eq) [side chain protection: Tyr (*t*-Bu); Cys (Trt); Lys (Boc); and Glu (*t*-Bu)], HOBt·H_2O (1 Eq), and WSCDI (1 Eq) were added to a solution of DMAE hydrochloride in dimethylformamide at 0°C. The mixture was stirred for 12 h at room temperature and extracted with ethyl acetate. The extract was washed with saturated citric acid, saturated $NaHCO_3$, and brine and dried over $MgSO_4$. Concentration under reduced pressure followed by flash chromatography over silica gel gave the amide compound. Deprotection of the resulting amide with 4 M HCl-dioxane for 2 h at room temperature followed by purification through reversed-phase-HPLC (H_2O-CH_3CN containing 0.1% TFA) gave the desired midodrine derivative (1:1 mixture of diastereomers) as TFA salts (two steps, ~50–80% yield). All compounds were characterized by ^{1}H NMR and electrospray ionization-mass spectrometry.

Cell Culture. Caco-2 cells obtained from the American Type Culture Collection (ATCC HTB37) were maintained by serial passage in plastic culture dishes as described previously (Irie et al., 2001). To measure the uptake of midodrine from the apical side, Caco-2 cells were seeded on 35-mm plastic dishes (2×10^5 cells/dish, 2 ml of culture medium). The cell monolayers were given fresh culture medium every 2 to 4 days and were used on the 14th or 15th day for experiments.

Uptake Experiments with Cell Monolayers. The uptake of [^{3}H]glycylsarcosine was measured as described previously (Terada et al., 1997). In experiments using midodrine, DMAE, and DMAE amino acid derivatives, the extraction solution (water/acetonitrile, 50:50) was added to the cells after the uptake period. On standing for 1 h at room temperature, the solutions were centrifuged and the supernatants were filtered through a Millipore filter (SGJVL, 0.22 μm; Millipore Corporation, Billerica, MA). The filtrates were analyzed by HPLC. Because midodrine and DMAE amino acid derivatives were partially metabolized to DMAE and each amino acid within Caco-2 cells and oocytes, the amounts of midodrine and

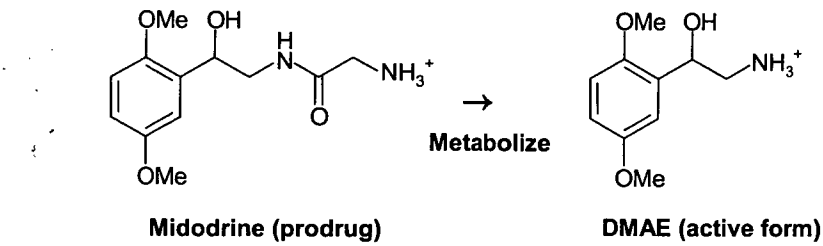

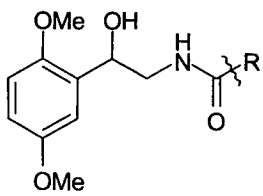

DMAE Amino Acid Derivatives

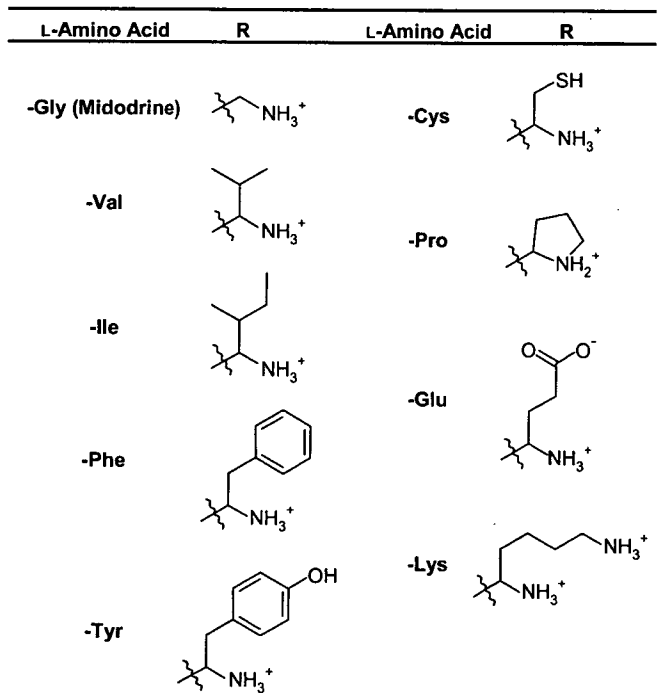

Fig. 1. Structures of midodrine, DMAE, and DMAE amino acid derivatives.

DMAE amino acid derivatives taken up were calculated as the sum of the amounts of the unchanged form and DMAE.

Simulation. A 14-state model of PEPT1, which we recently constructed (Irie et al., 2005), was used to simulate the pH profiles of midodrine and glutamate derivative of DMAE.

Uptake Experiments with *Xenopus* Oocytes. The synthesis and injection of cRNA were performed as described previously (Terada et al., 1996). The uptake of midodrine and DMAE was examined as reported with slight modifications (Saito et al., 1995). In brief, the uptake reaction was initiated in a 24-well plate by incubating the oocytes in 500 μl of uptake buffer, pH 6.0 (96 mM NaCl, 2 mM KCl, 1.8 mM $CaCl_2$, 1 mM $MgCl_2$, and 5 mM MES, pH 6.0, or HEPES, pH 7.4) containing 1 mM midodrine or DMAE for 1 h at room temperature. At the end of the uptake period, oocytes were washed five times in 1.5 ml of ice-cold uptake buffer, pH 7.4, and were transferred to a 1.5-ml tube. The oocytes were homogenized in 0.2 ml of extraction solution (water/acetonitrile, 50:50). The homogenates were centrifuged at 10,000 rpm for 5 min, and supernatants were filtered through a Millipore filter SGJVL (0.45 μM). The filtrates were analyzed by HPLC.

In Vivo Experiments. Experiments in vivo were performed as described previously (Pan et al., 2003). In brief, rats were anesthetized with sodium pentobarbital (50 mg/kg). The femoral artery was cannulated with a polyethylene tube (SP-31; Natsume Seisakusho, Tokyo, Japan) for blood sampling. For the intraintestinal administration of midodrine, the abdominal cavity of rats was opened via a midline incision, and the upper site of the duodenum was exposed to administer the drug. Midodrine was injected into the lumen of the duodenum at a dose of 2.91 mg/kg. Blood samples were collected from the femoral artery at 1, 5, 10, 15, 30, 45, 60, 90, and 120 min after the end of the injection. The blood samples were centrifuged at 14,000 rpm for 3 min, and 100 μl of plasma was deproteinized by adding 200 μl of methanol. The samples were centrifuged at 14,000 rpm for 3 min, and supernatants were filtered through a Millipore filter (SGJVL, 0.45 μm). The filtrates were analyzed by HPLC.

Analytical Methods. The uptake of midodrine and DMAE by Caco-2 cells and oocytes was measured simultaneously using high-performance liquid chromatograph LC-10AD_{SP} (Shimadzu Co., Kyoto, Japan) equipped with an SPD-10A_{VP} variable wavelength UV detector (Shimadzu Co.) and an integrator (Chromatopac C-R8A; Shimadzu Co.) under the following conditions: column, TSK-gel ODS 80TM (4.6 mm i.d. × 150; Tosoh Co., Tokyo, Japan); mobile phase, 1% SDS/phospholic acid/acetonitrile, 600:1:400; flow rate, 0.8 ml/min; wavelength, 290 nm; injection volume, 50 μl; and temperature, 50°C for midodrine, DMAE, and DMAE amino acid derivatives, except for a lysyl derivative of DMAE: mobile phase, water, and acetonitrile, both containing 0.1% (v/v) TFA, linear gradient of acetonitrile in water 10 to 40% over 30 min; flow rate, 1.0 ml/min; wavelength, 220 nm; injection volume, 50 μl; and temperature, 40°C for a lysyl derivative of DMAE.

Data Analysis. Each experimental point represents the mean ± S.E. of three to nine measurements from one to three separate experiments. Data from uptake experiments were analyzed statistically by a one-way analysis of variance followed by Sheffé's test. Kinetic parameters of the DMAE plasma concentration were statistically compared using a nonpaired t test.

Results

Effect of Midodrine on [^{3}H]Glycylsarcosine Uptake by Caco-2 Cells. To assess the interaction of midodrine with PEPT1, we examined the inhibitory effect of midodrine on [^{3}H]glycylsarcosine uptake by Caco-2 cells. As shown in Fig. 2A, [^{3}H]glycylsarcosine uptake was inhibited by midodrine in a concentration dependent manner, and the IC_{50} value was calculated at 2.8 ± 0.1 mM.

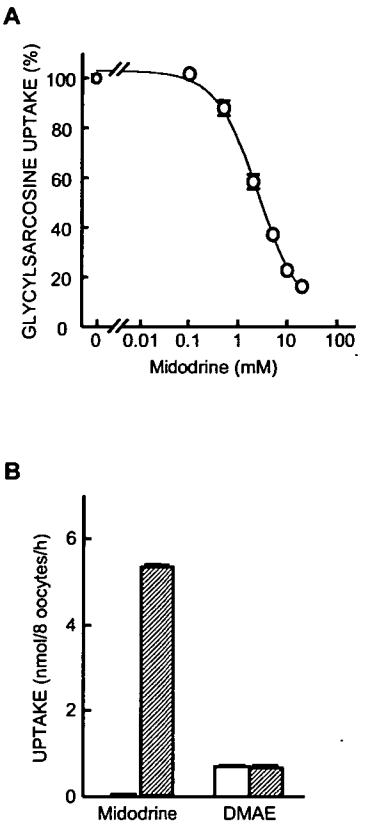

Fig. 2. A, effect of midodrine on [^{3}H]glycylsarcosine uptake by Caco-2 cells. The cell monolayers were incubated at 37°C for 15 min with 25 μM [^{3}H]glycylsarcosine, pH 6.0, in the presence of various concentrations of midodrine. After the incubation, the radioactivity of dissolved cells was measured. Each point represents the mean ± S.E. of three independent monolayers. The IC_{50} value was calculated from three separate experiments. B, uptake of midodrine and DMAE by oocytes expressing PEPT1. Water-injected (open column) or PEPT1-expressing (hatched column) oocytes were incubated at 37°C for 1 h with 1 mM midodrine or DMAE, pH 6.0. The amounts of midodrine and DMAE in the solubilized oocytes were measured by HPLC. Each column represents the mean ± S.E. of three experiments. Each experiment was performed with eight oocytes.

Uptake of Midodrine and DMAE by Oocytes Expressing PEPT1. To confirm the midodrine transport by PEPT1, we measured the uptake of midodrine and DMAE by PEPT1-expressing oocytes. As shown in Fig. 2B, the uptake of midodrine was markedly increased in PEPT1-expressing oocytes compared with water-injected oocytes. In contrast, no PEPT1-mediated transport of DMAE was observed.

Uptake of Midodrine and DMAE by Caco-2 Cells. To investigate the transport and metabolism of midodrine in the intestinal epithelial cells, uptake experiments were performed using Caco-2 cells. Figure 3A shows the time course of midodrine and DMAE uptake by Caco-2 cells. As shown in Fig. 3A, more midodrine than DMAE was taken up at each time point. After 1 h of incubation in Caco-2 cells, ~35% midodrine was metabolized to DMAE (Fig. 3B)

Transport Characteristics of Midodrine in Caco-2 Cells. Figure 4A shows the effect of various compounds on midodrine uptake in Caco-2 cells. PEPT1-dependent part of midodrine uptake was nearly completely inhibited by PEPT1 substrates, but not by glycine. As shown in Fig. 4B, midodrine uptake by Caco-2 cells was saturable, and the apparent Michaelis-Menten constant (K_m) value was calculated at 4.5 ± 1.3 mM.

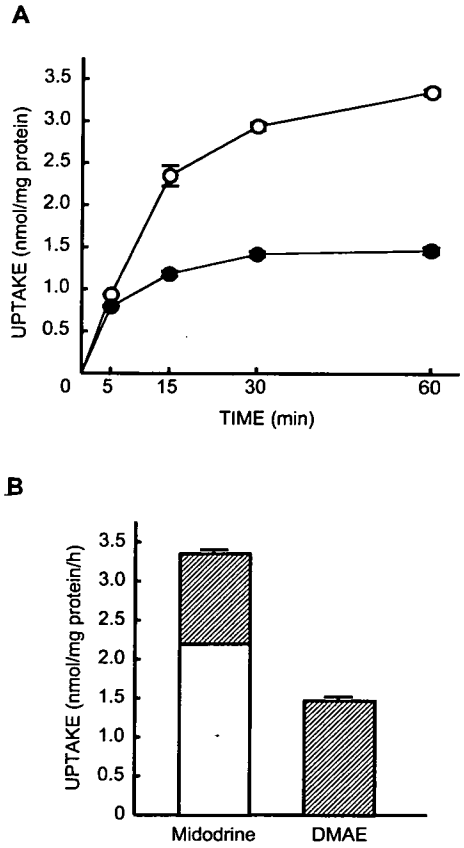

Fig. 3. A, time course of midodrine and DMAE uptake by Caco-2 cells. The cell monolayers were incubated at 37°C for the periods indicated with 0.5 mM midodrine or DMAE, pH 6.0. After the incubation, the amounts of midodrine (○) and DMAE (●) extracted from the cell monolayers were measured by HPLC. Each point represents the mean ± S.E. of three independent monolayers. B, metabolism of midodrine in Caco-2 cells after 1-h uptake. Open and hatched columns represent midodrine and DMAE, respectively. Each column represents the mean ± S.E. of three independent monolayers.

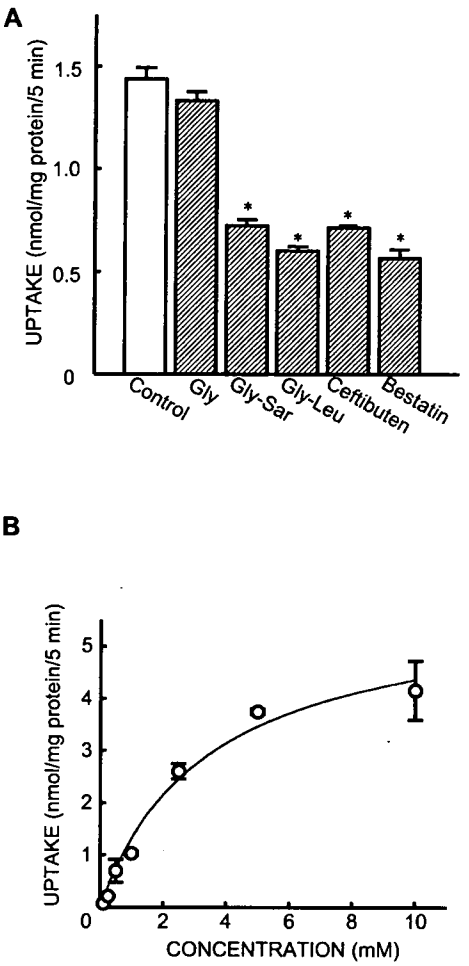

Fig. 4. A, effect of various compounds on midodrine uptake by Caco-2 cells. The cell monolayers were incubated at 37°C for 5 min with 0.5 mM midodrine, pH 6.0, in the absence or presence of each inhibitor (10 mM). After the incubation, the amounts of midodrine and DMAE extracted from the cell monolayers were measured by HPLC. Each column represents the mean ± S.E. of three independent monolayers. *, $P < 0.05$, significantly different from the control. B, concentration dependence of midodrine uptake by Caco-2 cells. Nonspecific uptake was evaluated by measuring midodrine uptake in the presence of 50 mM glycylleucine, and the results are shown after correction for the nonsaturable component. The cell monolayers were incubated at 37°C for 5 min with various concentration of midodrine, pH 6.0. After the incubation, the amounts of midodrine and DMAE extracted from the cell monolayers were measured by HPLC. Each point represents the mean ± S.E. of three independent monolayers. The K_m value was calculated from three separate experiments.

Absorption of Midodrine from Rat Intestine. To confirm the involvement of PEPT1 in the transport of midodrine in vivo, we performed a pharmacokinetic analysis. Figure 5 shows the time course of DMAE plasma concentration after the intraintestinal administration of midodrine in rats. The concentration peaked 5 min after the intraintestinal administration, indicating that the absorption of midodrine was very rapid. Midodrine absorption was inhibited in the presence of cyclacillin, a high-affinity substrate of PEPT1, until 30 min postadministration. The estimated pharmacokinetic parameters are summarized in Table 1. The area under the blood concentration-time curve for 30 min (AUC_{0-30}) and the maximal concentration in the presence of cyclacillin were reduced significantly compared with the control values, and the time to maximal concentration (t_{max}) was significantly longer than the control.

Uptake of DMAE Amino Acid Derivatives in Caco-2 Cells. To examine which amino acid modification of midodrine is suitable for interaction with PEPT1, we synthesized various DMAE-L-amino acid derivatives DMAE-X (X: -Val, -Ile, -Phe, -Tyr, -Cys, -Pro, -Glu, and -Lys), in which the glycine residue is replaced by other amino acids (Fig. 1). We measured the uptake of these derivatives in Caco-2 cells in the absence or presence of the excess glycylsarcosine (Fig. 6). DMAE-Phe uptake was greatest but was not inhibited by the glycylsarcosine. DMAE-Val, -Ile, -Tyr, -Cys, -Glu, and -Lys uptake was roughly equal to midodrine uptake, but the excess glycylsarcosine did not have a significant inhibitory effect in the case of DMAE-Ile and -Lys. DMAE-Pro uptake by Caco-2 cells was low and not inhibited by the excess glycylsarcosine. Furthermore, using in vitro everted sacs of the rat small intestine, we examined the stability of three kinds of derivatives (DMAE-Gly, -Val, and -Phe) at the mucosal surface. The ratio of unchanged form at the mucosal side after 1 h of incubation was as follows: DMAE-Gly (95%), -Val (47%), and -Phe (0.7%), suggesting that DMAE-Gly (midodrine) is the most stable derivative among the tested compounds.

pH Dependence of Midodrine and DMAE-Glu Uptake by Caco-2 Cells. Figure 7A shows the pH dependence of midodrine and DMAE-Glu uptake by Caco-2 cells. In contrast

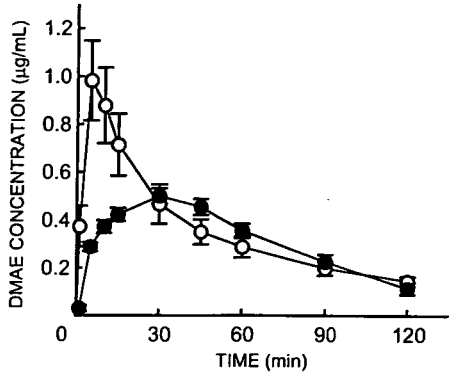

Fig. 5. DMAE plasma concentration after intraintestinal administration in the absence or presence of cyclacillin. After intraintestinal administration at a dose of 2.91 mg/kg midodrine and in the absence (○) or presence (●) of 6.85 mg/kg cyclacillin, blood samples were collected at the times indicated. The blood samples were determined by HPLC. Each point represents the mean ± S.E. of six rats.

TABLE 1

Pharmacokinetic parameters of the DMAE plasma concentration in the absence or presence of cyclacillin after intraintestinal administration

Each value represents the mean ± S.E. of six rats.

	$AUC_{0-30\ min}$	$AUC_{0-120\ min}$	C_{max}	t_{max}
	μg·min/ml		*μg/ml*	*min*
Control	20.4 ± 3.5	43.6 ± 7.0	1.01 ± 0.18	5.8 ± 0.8
+Cyclacillin	11.3 ± 0.7*	38.1 ± 3.0	0.51 ± 0.03*	35.0 ± 3.2*

C_{max}, maximal concentration.
*$P < 0.01$, significantly different from the control.

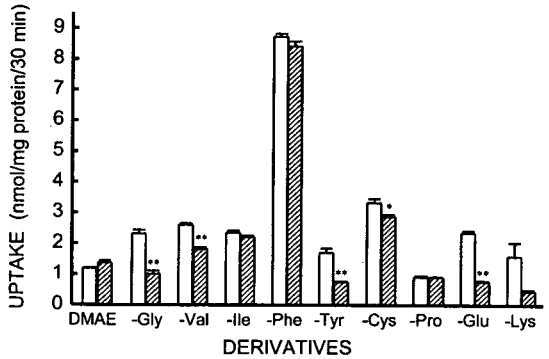

Fig. 6. Uptake of DMAE amino acid derivatives in Caco-2 cells. The cell monolayers were incubated at 37°C for 30 min with 0.5 mM of each DMAE amino acid derivative in the absence (opened column) or presence (hatched column) of 10 mM glycylsarcosine. After the incubation, the amounts of DMAE amino acid derivatives extracted from the cell monolayers were measured by HPLC. Each column represents the mean ± S.E. of three independent monolayers. *, $P < 0.05$; **, $P < 0.01$, significantly different from the control.

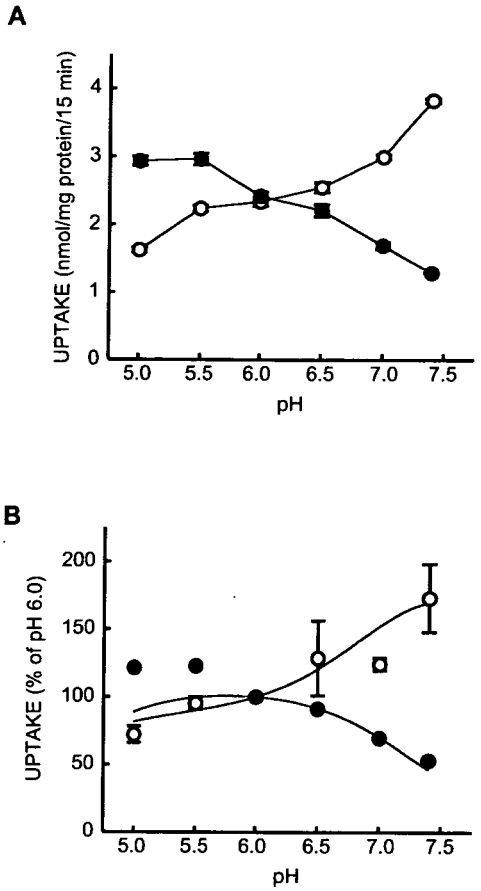

Fig. 7. A, pH dependence of midodrine (○) and DMAE-Glu (●) uptake by Caco-2 cells. The cell monolayers were incubated at 37°C for 15 min with 0.5 mM midodrine or DMAE-Glu, pH 6.0. After the incubation, the amounts of midodrine, DMAE-Glu, and DMAE extracted from the cell monolayers were measured by HPLC. Each point represents the mean ± S.E. of three independent monolayers. B, simulation of pH dependence of midodrine (○) and DMAE-Glu (●) uptake by Caco-2 cells. The rates of uptake value at pH 6.0 were derived from the uptake values in Fig. 6A. The pH profiles of midodrine and DMAE-Glu uptake were delineated by simulation (curve). Four dissociation constants (in micromolars) of midodrine and DMAE-Glu on the exterior side ($K_{d,\ Soc1}$, $K_{d,\ Soc2}$, $K_{d,\ Son}$, and $K_{d,\ Soa}$) were defined as follows: $K_{d,\ Soc1} = 1500$, $K_{d,\ Soc2} = 120$, $K_{d,\ Son} = 2000$, $K_{d,\ Soa} = 2000$, $K_{d,\ Soc1} = 500$, $K_{d,\ Soc2} = 500$, $K_{d,\ Son} = 300$, and $K_{d,\ Soa} = 2000$, respectively.

to neutral substrates, the cationic midodrine was taken up extensively at alkaline pH. This pH profile was similar to that of the cationic dipeptides transported by PEPT1 (Mackenzie et al., 1996). On the other hand, the pH dependence of DMAE-Glu (neutral) uptake was high at acidic pH. Recently, we constructed a 14-state model of PEPT1 and reproduced the pH profiles of various charged substrates (Irie et al., 2005). The pH profile of midodrine as well as DMAE-Glu was reproduced by our 14-state model of PEPT1 (Fig. 7B). In the simulation, the uptake of midodrine and DMAE-Glu was calculated every 0.01 pH units. Four dissociation constants of midodrine and DMAE-Glu on the exterior side ($K_{d,\ Soc1}$, $K_{d,\ Soc2}$, $K_{d,\ Son}$, and $K_{d,\ Soa}$) were recalculated based on our 14-state model (Irie et al., 2005).

Discussion

Midodrine is an oral drug that acts as a selective α1-receptor agonist and the medication of choice for treating orthostatic hypotension in the elderly (Mukai and Lipsitz, 2002). Furthermore, this drug is beneficial in preventing or ameliorating the symptoms of intradialytic hypotension (Prakash et al., 2004). There are many reports regarding the pharmacological and clinical effects of midodrine, but its pharmacokinetic properties, especially the mechanism behind its intestinal absorption, have not been elucidated. In the present study, we demonstrated for the first time that midodrine was transported by PEPT1 in vitro and in vivo. Because PEPT1 can transport various peptide-like drugs, such as β-lactam antibiotics and antiviral drugs, and also mediates the cellular uptake of dipeptides and tripeptides derived from ingested proteins, there is potential for drug/

drug interaction and/or drug/food interaction during therapy with midodrine.

Previously, Beauchamp et al. (1992) evaluated the bioavailability of 18 ester compounds of acyclovir and found that the L-valyl ester derivative had the best bioavailability followed by the L-isoleucyl, L-alanyl, and glycyl ester derivatives. Thereafter, these amino acid preferences were demonstrated to be related to the affinity for PEPT1 (Sawada et al., 1999). Thus, for amino acid ester modification, L-valine may be a suitable target for converting a poorly absorbed drug into a substrate of PEPT1. On the other hand, for amino acid modification of a peptide bond, there is little information available on which amino acids provide for high-affinity interaction with PEPT1 and resistance against enzymatic degradation. In the present study, we demonstrated that the derivatives with -Gly, -Val, -Tyr, -Cys, and -Glu were suggested to be interacted with PEPT1, but those with -Ile, -Phe, -Pro, and -Lys did not (the lack of significant difference in the case of -Lys may be caused by the unusually high scatter). Large amounts of DMAE-Phe were accumulated in Caco-2 cells, but this derivative showed extremely low stability in the rat small intestine. These findings suggest that DMAE-Phe may not be appropriate for a prodrug for targeting PEPT1 and improving the intestinal absorption in vivo. On the other hand, DMAE-Gly (midodrine) was high stability and can be recognized by PEPT1. Although we did not perform a detailed analysis, overall, our results suggest that Gly modification of DMAE by a peptide bond is appropriate for the preparation of a prodrug for DMAE. Further studies are needed to define the amino acids suitable for targeting PEPT1 in peptide bond-based modifications.

It has been reported that pH dependences of neutral (Inui et al., 1992; Saito and Inui, 1993; Terada et al., 1999; Kennedy et al., 2002) and anionic (Matsumoto et al., 1995) substrates of PEPT1 show different profiles. The pH dependence of cationic substrates determined by measuring evoked current is also different from neutral and anionic substrates (Mackenzie et al., 1996). Midodrine almost exists as a cation at pH 5.0 to 7.4, because its dissociation constant (p*K*a) is 7.96. As shown in Fig. 7A, midodrine uptake by PEPT1 gradually increased as the pH rose from 5.0 to 7.4. This pH profile clearly differs from that of a neutral substrate, such as glycylsarcosine, or an anionic substrate, such as ceftibuten. In contrast, the pH profile of DMAE-Glu, which mainly exists as a neutral substrate from pH 5.0 to 7.4, was similar to that of glycylsarcosine. Recently, based on the presumed recognition patterns of PEPT1 for neutral and charged substrates, we constructed a 14-state model of PEPT1 and reproduced the pH profiles of various charged substrates (Irie et al., 2005). In this model, we hypothesized two mechanisms for the transport of cationic substrates, namely, that the transport of cationic substrate occurs with or without H^+. Therefore, the transport of cationic substrates is assumed to be altered by the degree of contribution of the two pathways. In the previous study, we could not simulate the pH profile of cationic substrates, because there is little known regarding the transport characteristics of cationic substrates of PEPT1. The present simulation revealed that the pH profile of midodrine as well as DMAE-Glu was reproduced by our 14-state model of PEPT1 (Fig. 7B), suggesting that our model can be applied to cationic as well as neutral substrates.

In conclusion, we have demonstrated that midodrine, but not DMAE, is recognized by PEPT1 and that this recognition improves the oral bioavailability of DMAE. In addition, the transport of DMAE amino acid derivatives via PEPT1 depends on the amino acids modified. These findings suggested that modifying not only the L-valyl ester but also the glycyl peptide of poorly absorbed drugs, which are targeted to intestinal PEPT1, is useful for improving of the intestinal absorption of drugs.

References

Beauchamp LM, Orr GF, de Miranda P, Burnette T, and Krenitsky (1992) Amino acid ester prodrugs of acyclovir. *Antiviral Chem Chemother* **3**:157–164.

Daniel H (2004) Molecular and integrative physiology of intestinal peptide transport. *Annu Rev Physiol* **66**:361–384.

Daniel H and Kottra G (2004) The proton oligopeptide cotransporter family SLC15 in physiology and pharmacology. *Pflueg Arch Eur J Physiol* **447**:610–618.

Han H, de Vrueh RL, Rhie JK, Covitz KM, Smith PL, Lee CP, Oh DM, Sadée W, and Amidon GL (1998) 5′-Amino acid esters of antiviral nucleosides, acyclovir and AZT are absorbed by the intestinal PEPT1 peptide transporter. *Pharm Res (NY)* **15**: 1154–1159.

Inui K and Terada T (1999) Dipeptide transporters, in *Membrane Transporters as Drug Targets* (Amidon GL and Sadée W eds) pp 269–288, Academic/Plenum Publishers, New York.

Inui K, Yamamoto M, and Saito H (1992) Transepithelial transport of oral cephalosporins by monolayers of intestinal epithelial cell line Caco-2: specific transport systems in apical and basolateral membranes. *J Pharmacol Exp Ther* **261**:195–201.

Irie M, Terada T, Katsura T, Matsuoka S, and Inui K (2005) Computational modeling of H^+-coupled peptide transport via human PEPT1. *J Physiol (Lond)* **565**:429–439.

Irie M, Terada T, Sawada K, Saito H, and Inui K (2001) Recognition and transport characteristics of nonpeptidic compounds by basolateral peptide transporter in Caco-2 cells. *J Pharmacol Exp Ther* **298**:711–717.

Kennedy DJ, Leibach FH, Ganapathy V, and Thwaites DT (2002) Optimal absorptive transport of the dipeptide glycylsarcosine is dependent on functional Na^+/H^+ exchange activity. *Pflueg Arch Eur J Physiol* **445**:139–146.

Mackenzie B, Fei YJ, Ganapathy V, and Leibach FH (1996) The human intestinal H^+/oligopeptide cotransporter hPEPT1 transports differently-charged dipeptides with identical electrogenic properties. *Biochim Biophys Acta* **1284**:125–128.

Matsumoto S, Saito H, and Inui K (1995) Transport characteristics of ceftibuten, a new cephalosporin antibiotic, via the apical H^+/dipeptide cotransport system in human intestinal cell line Caco-2: regulation by cell growth. *Pharm Res (NY)* **12**:1483–1487.

Mukai S and Lipsitz LA (2002) Orthostatic hypotension. *Clin Geriatr Med* **18**:253–268.

Pan X, Terada T, Okuda M, and Inui K (2003) Altered diurnal rhythm of intestinal peptide transporter by fasting and its effects on the pharmacokinetics of ceftibuten. *J Pharmacol Exp Ther* **307**:626–632.

Prakash S, Garg AX, Heidenheim AP, and House AA (2004) Midodrine appears to be safe and effective for dialysis-induced hypotension: a systematic review. *Nephrol Dial Transplant* **19**:2553–2558.

Saito H and Inui K (1993) Dipeptide transporters in apical and basolateral membranes of the human intestinal cell line Caco-2. *Am J Physiol* **265**:G289–G294.

Saito H, Okuda M, Terada T, Sasaki S, and Inui K (1995) Cloning and characterization of a rat H^+/peptide cotransporter mediating absorption of beta-lactam antibiotics in the intestine and kidney. *J Pharmacol Exp Ther* **275**:1631–1637.

Sawada K, Terada T, Saito H, Hashimoto Y, and Inui K (1999) Recognition of L-amino acid ester compounds by rat peptide transporters PEPT1 and PEPT2. *J Pharmacol Exp Ther* **291**:705–709.

Sugawara M, Huang W, Fei YJ, Leibach FH, Ganapathy V, and Ganapathy ME (2000) Transport of valganciclovir, a ganciclovir prodrug, via peptide transporters PEPT1 and PEPT2. *J Pharm Sci* **89**:781–789.

Terada T and Inui K (2004) Peptide transporters: structure, function, regulation, and application for drug delivery. *Curr Drug Metab* **5**:85–94.

Terada T, Saito H, Mukai M, and Inui K (1996) Identification of the histidine residues involved in substrate recognition by a rat H^+/peptide cotransporter, PEPT1. *FEBS Lett* **394**:196–200.

Terada T, Saito H, Mukai M, and Inui K (1997) Recognition of beta-lactam antibiotics by rat peptide transporters, PEPT1 and PEPT2, in LLC-PK_1 cells. *Am J Physiol* **273**:F706–F711.

Terada T, Sawada K, Saito H, and Inui K (1999) Functional characteristics of basolateral peptide transporter in the human intestinal cell line Caco-2. *Am J Physiol* **276**:G1435–G1441.

Yang CY, Dantzig AH, and Pidgeon C (1999) Intestinal peptide transport systems and oral drug availability. *Pharm Res (NY)* **16**:1331–1343.

Address correspondence to: Professor Ken-ichi Inui, Department of Pharmacy, Kyoto University Hospital, Sakyo-ku, Kyoto 606-8507, Japan. E-mail: inui@kuhp.kyoto-u.ac.jp

The PDZ domain protein PDZK1 interacts with human peptide transporter PEPT2 and enhances its transport activity

R Noshiro[1,2,4], N Anzai[1,4], T Sakata[1,2], H Miyazaki[1], T Terada[3], HJ Shin[1], X He[1], D Miura[1], K Inui[3], Y Kanai[1] and H Endou[1,2]

[1]*Department of Pharmacology and Toxicology, Kyorin University School of Medicine, Mitaka, Tokyo, Japan;* [2]*Fuji Biomedix Co. Ltd, Chuo-ku, Tokyo, Japan and* [3]*Department of Pharmacy, Kyoto University Hospital, Sakyo-ku, Kyoto, Japan*

The proton-coupled peptide transporter PEPT2 (*SLC15A2*) mediates the high-affinity low-capacity transport of small peptides as well as various oral peptide-like drugs in the kidney. In contrast to its well-characterized transport properties, there is less information available on its regulatory mechanism, although the interaction of PEPT2 to the PDZ (PSD-95, DglA, and ZO-1)-domain protein PDZK1 has been preliminarily reported. To examine whether PDZK1 is a physiological partner of PEPT2 in kidneys, we started from a yeast two-hybrid screen of a human kidney cDNA library with the C-terminus of PEPT2 (PEPT2 C-terminus (PEPT2-CT)) as bait. We could identify PDZK1 as one of the positive clones. This interaction requires the PDZ motif of PEPT2-CT detected by a yeast two-hybrid assay, *in vitro* binding assay and co-immunoprecipitation. The binding affinities of second and third PDZ domains of PDZK1 to PEPT2-CT were measured by surface plasmon resonance. Co-immunoprecipitation using human kidney membrane fraction and localization of PEPT2 in renal apical proximal tubules revealed the physiological meaning of this interaction in kidneys. Furthermore, we clarified the mechanism of enhanced glycylsarcosine (Gly-Sar) transport activity in PEPT2-expressing HEK293 cells after the PDZK1 coexpression. This augmentation was accompanied by a significant increase in the V_{max} of Gly-Sar transport via PEPT2 and it was also associated with the increased surface expression level of PEPT2. These results indicate that the PEPT2-PDZK1 interaction thus plays a physiologically important role in both oligopeptide handling as well as peptide-like drug transport in the human kidney.

Kidney International (2006) **70,** 275–282. doi:10.1038/sj.ki.5001522; published online 31 May 2006

KEYWORDS: oligopeptides; oligopeptide transporter; PEPT2; PDZ; PDZK1

Correspondence: *Y Kanai, Department of Pharmacology and Toxicology, Kyorin University School of Medicine, 6-20-2 Shinkawa, Mitaka, Tokyo 181-8611, Japan. E-mail: ykanai@kyorin-u.ac.jp*

[4]These authors contributed equally to this work.

Received 6 August 2005; revised 21 February 2006; accepted 8 March 2006; published online 31 May 2006

Proton-coupled peptide transporters play an important role in the maintenance of nutrition by mediating the transport of di- and tripeptides across the brush border (apical) membranes of the small intestine and kidney. In addition, peptide transporters function as drug transporters for peptide-like drugs, including β-lactam antibiotics and angiotensin converting enzyme inhibitors.[1–3] Two proton-coupled oligopeptide transporters, PEPT1 and PEPT2, have previously been cloned in rabbits,[4–6] rats[7–9] and humans.[10–12] PEPT1 was thus shown to be a high-capacity, low-affinity transporter that is expressed mainly in small intestine and, to smaller extent, in kidneys. It has been shown to play an essential role in the absorption of small peptides arising from the digestion of dietary proteins. In contrast, PEPT2 was found to be a low-capacity, high-affinity transporter that is expressed in the kidneys. In rats, Pept1 and Pept2 are sequentially expressed: Pept1 is located in the early segment and Pept2 is in the late segment of the proximal tubules.[13] In addition, both Pept1 and Pept2 are localized in the apical membranes of renal proximal tubule in rats.[14,15] Although both transporters are expressed in the kidney, PEPT2 is thought to play a dominant role in the conservation of peptide-bound amino acids. Recently, Rubio-Aliaga *et al.*[16] have reported on the impaired renal reabsorption of peptide-bound amino acids in animals lacking Pept2.

Although the transport properties and characteristics of substrate recognition for PEPT2 have been well documented, there is less information available on PEPT2 regulation. Takahashi *et al.*[17] reported a pronounced upregulation of Pept2 mRNA and protein expression in 5/6 nephrectomized rats 2 weeks after surgery and the downregulation of its mRNA 16 weeks after surgery.[18] Wenzel *et al.*[19] demonstrated that the activation of signaling pathways involving protein kinase C changes the kinetic property of pig Pept2 in a renal cell line. Recently, Bravo *et al.*[20] demonstrated a strong inhibitory effect of EGF on the rat Pept2 transport capacity. However, the modulation of the PEPT2 function by its associated protein(s) still remains unclear.

In recent years, several PDZ domain proteins, such as NHERF1/EBP50, NHERF2/E3KARP, and PDZK1, have been identified in kidneys and thus have been suggested to be involved in the stabilization, targeting, and regulation of their binding partner.[21–24] The PDZ (PSD-95, DglA, and ZO-1)-binding domains have been identified in various proteins and they are considered to be modular protein–protein recognition domains that play a role in protein targeting and protein complex assembly.[25–27] This domain binds to proteins containing the tripeptide motif $(S/T)-X-\emptyset$ (X = any residue and $\emptyset$ = a hydrophobic residue) at their C-termini.[27] As Russel *et al.*[28] mentioned, PEPT2 is localized to the apical membrane and has C-terminal amino-acid sequences that match the PDZ-binding motif (T-K-L), in a manner similar to that of other apical organic anion transporters, such as MRP2/4, NPT1, Oatp1, Oat-k1/k2; thus, indicating that PEPT2 most likely binds to certain PDZ domain proteins. We have recently identified that the urate/anion exchanger URAT1, which has a PDZ motif at its C-terminus (T-Q-F), interacts with PDZK1.[29] Interestingly, both URAT1 and PEPT2 are expressed at the apical membrane of renal proximal tubules and they are considered to function in a reabsorptive pathway for endogenous organic anions (urate[30] and oligopeptides,[1–3] respectively). It is likely that these transporters bind to either the same or other PDZ domain protein(s) via its PDZ-motif.

Very recently, Kato *et al.*[31] examined the interaction between xenobiotic transporters including PEPT2, and PDZ proteins including PDZK1. PDZK1, originally identified as a protein that interacts with MAP17, a membrane-associated protein,[32] has been reported to interact with several membrane proteins through its PDZ domain.[33] Using coexpression of PEPT2 C-terminus (PEPT2-CT) and PDZK1 in yeast, a possible interaction was demonstrated in the artificial condition. Because they solely rely on data from *in vitro* binding assays and did not provide any evidence that this interaction truly occurs in proteins expressed from the endogenous tissue, we performed yeast two-hybrid screening against a human kidney cDNA library using PEPT2-CT as bait and thus characterized this interaction in order to identify PDZK1 as a physiological binding partner of PEPT2.

RESULTS

Identification of PDZK1 by yeast two-hybrid library screening

In an attempt to isolate PEPT2-interacting protein(s) from the endogenous genes, we performed yeast two-hybrid screening against a cDNA library constructed from the human adult kidney using the PEPT2-CT as bait. From the 8.7×10^6 transformants screened, we obtained 64 positive clones. One of these clones had a sequence identical to a portion of the human PDZK1 gene.[32] We could not detect any interactions between PEPT2-CT and any other PDZ proteins that are expressed at and/or beneath the apical membrane of proximal tubules including NHERF1/EBP50, NHERF2/E3KARP, and IKEPP[34–37] (data not shown).

C-terminal PDZ motif of PEPT2 is necessary for PDZK1 interaction

To identify the region of PEPT2 that interacts with PDZK1, we constructed three mutant baits. A bait (PEPT2-CTd3) which lacks the last three residues of PEPT2, which play a crucial role in PDZ domain recognition. Two other baits (L729A and T727A), the extreme C-terminal leucine (0 position) or threonine (−2 position) of PEPT2 was replaced by alanine, which was expected to abolish the PDZ interactions.[38] These three baits did not interact with PDZK1 (Figure 1a). Therefore, the binding through PEPT2-CT suggests that the PDZ motif of PEPT2 is the site of interaction with PDZK1.

The interaction specificity between PDZK1 and PEPT2-CT was confirmed by a yeast two-hybrid assay using a bait that had the C-terminus of another human peptide transporter, PEPT1. PDZK1 did not interact with PEPT1-CT which lacks a PDZ motif (K-Q-M) (Figure 1b).

Interaction of PDZK1 individual PDZ domains with PEPT2-CT

PDZK1 possesses four PDZ domains which facilitate the assembly of protein complexes when target proteins bind via their C-terminal PDZ motifs. To determine the possible interactions of PEPT2-CT with the PDZ domains of PDZK1, we produced prey vectors, with each containing one of the individual PDZ domains (PDZ domain 1 (PDZ1), PDZ2, PDZ3, and PDZ4) from PDZK1. The interaction with the

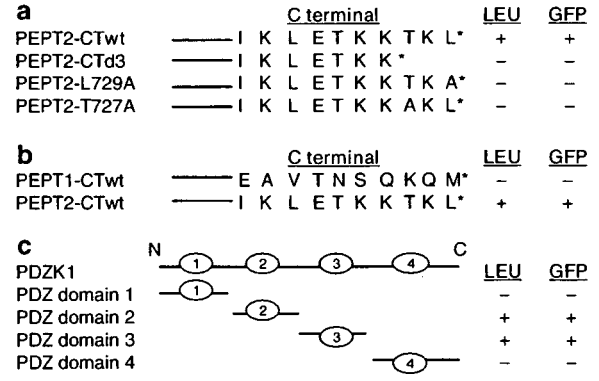

Figure 1 | Specificity of PDZK1 interaction with C-termini of PEPT2 in yeast two-hybrid system. (**a**) PDZK1 specifically interacted with the wt PEPT2 C-terminus but not with the C-terminal mutants L729A, T727A, and d727–729 (d3) of PEPT2. (**b**) Full-length PDZK1 interacting with the intracellular C-terminus of PEPT2 but not with that of PEPT1. (**c**) The wt PEPT2 C-terminus bait interacts with prey containing either the second or third PDZ domains of PDZK1 (PDZ2, PDZ3). The specificity of the prey containing a single PDZ domain of PDZK1 for the PEPT2 bait was confirmed by the absence of growth associated with the PEPT2 d3 mutant baits. The bars represent the approximate length of the baits, and the sequence of the last 10 amino acids is shown. pJG4-5 with PDZK1 cDNA expression cassette is under the control of the GAL1 promoter, such that library proteins are expressed in the presence of galactose (Gal) but not glucose (Glu). The system used for the yeast two-hybrid screen includes the reporter genes LEU2 and GFP, which replace the commonly used classical *lacZ* gene and allow a fast and easy detection of positive clones with long-wave UV. The results from the growth assay and GFP fluorescence are indicated on the right.